Deltares

Enabling Delta Life

Sediment exchange between the Wadden Sea and North Sea Coast

Modelling based on ASMITA

Deltares

Sediment exchange between the Wadden Sea and North Sea Coast

Modelling based on ASMITA

Zheng Wang
Q.J. Lodder

Deltares

Title
Sediment exchange between the Wadden Sea and North Sea Coast

Client	Project	Attribute	Pages
Rijkswaterstaat Water, Verkeer en Leefomgeving, UTRECHT	1220339-008	1220339-008-ZKS-0006	53

Keywords
Wadden Sea; Sea-level rise; Sediment import; ASMITA modelling.

Summary
The sediment exchange between the Dutch Wadden Sea and the North Sea coastal zone is simulated using the aggregated morphodynamic model ASMITA for four future sea-level rise scenarios: sea-level rise rate equal to 2, 4, 6 and 8 mm/y in 2100. The simulations have been carried out using existing ASMITA models for the various tidal inlets, as well as with updated models in which the parameter settings are based on the latest insights of the sediment exchanges through the tidal inlets. In addition, detailed background information of the ASMITA models is provided, and a theoretical analysis is carried to better understand the response of tidal basins to sea-level rise. This analysis supports the interpretation of the model results. It is concluded that the effect of accelerated sea-level rise on sediment import rates will not be noticeable before 2040, i.e. 20 year later than the start of the sea-level rise acceleration. The difference in the import rate between the four sea-level rise scenarios is limited until 2100, and no substantial increase of the import with respect to the present situation is expected until 2100.

References

Version	Date	Author	Initials	Review	Initials	Approval	Initials
0.1	Aug. 2019	Zheng Bing Wang		Edwin Elias		Frank Hoozemans	
1.1	Oct. 2019	Zheng Bing Wang	ZW	Edwin Elias	EE	Frank Hoozemans	

Status
final

Deltares

Title
Sediment exchange between the Wadden Sea and North Sea Coast

Client	Project	Attribute	Pages
Rijkswaterstaat Water, Verkeer en Leefomgeving, UTRECHT	1220339-008	1220339-008-ZKS-0006	53

Samenvatting
Sedimentuitwisseling tussen de (Noordzee) kustzone en de Waddenzee is belangrijk voor verschillende beheer- en beleidsaspecten. Voor het kustonderhoud t.b.v. de lang-termijn veiligheid tegen overstromingen is het van belang, omdat deze uitwisseling een belangrijke post in de sedimentbalans van het kustfundament vormt en de suppletiebehoefte langs de kust mede bepaald wordt door de uitwisseling. Voor de Waddenzee is het van belang, omdat de wadplaten van hoge ecologische waarde zijn en het wel of niet meegroeien van de wadplaten met zeespiegelstijging (ZSS) afhankelijk is van de sedimentuitwisseling. Het verkrijgen / verbeteren van het inzicht in de sedimentuitwisseling is daarom een belangrijke doelstelling voor de verschillende onderzoekprogramma's zoals Kustgenese 2, B&O Kust en KPP Morfologie Waddenzee.
Het doel van de voorliggende studie is te komen tot een voorspelling van de lange-termijn ontwikkelingen van de sedimentuitwisselingen door de zeegaten van de Waddenzee. Ten behoeve van het technische advies vanuit het Kustgenese 2 onderzoekprogramma over de sedimentuitwisselingen door de zeegaten worden de resultaten van deze studie gecombineerd met de resultaten van de studie naar de sedimentbalans van het Waddenzeegebied (Elias, 2019). De data-analyse van Elias (2019) levert inzicht in de huidige trend, terwijl deze modelleringsstudie inzicht geeft in (1) hoe de huidige trend verandert in de toekomst en (2) wat de verschillen in trend tussen de verschillende zeespiegelstijging (ZSS) scenario's zijn.
De voorspellingen wordt gedaan aan de hand van de ASMITA modellen voor de zes zeegaten (Zoutkamperlaag, Pinkegat, Amelander zeegat, Zeegat van het Vlie, Eierlandse Gat en Zeegat van Texel ofwel Marsdiep). Modelsimulaties zijn uitgevoerd over de periode 1970 - 2100 voor vier ZSS scenario's waarin de ZSS snelheid in 2100 gelijk is aan 2, 4, 6, en 8 mm/jaar. Het 2 mm/jaar scenario betreft voortzetting van de huidige ZSS. In de drie andere scenario's gaat de versnelling vanaf 2020 beginnen, met lineaire toename om de eindsnelheid te bereiken in respectievelijk 2050, 2060 en 2070.
De simulaties zijn eerst uitgevoerd met de bestaande modellen en daarna met de modellen die aan de hand van de inzichten uit de recente data-analyse (Elias, 2019) zijn aangepast. Een beschrijving van de ASMITA modelformulering samen met de achtergrondinformatie van het modelconcept is gegeven om inzicht te geven over de mogelijkheden en beperkingen van de gebruikte modellen. Verder is er een theoretische analyse uitgevoerd, en de inzichten daaruit zijn behulpzaam voor de interpretatie van de modelresultaten.
De theoretische analyse is uitgevoerd met een verder geaggregeerd model waarin het hele bekken als één element wordt beschouwd. Als morfologische toestandsvariabel in het model wordt de gemiddelde diepte van het bekken onder hoogwater gebruikt. Zonder ZSS is er een evenwichtsdiepte gedefinieerd die met de empirische relaties kan worden berekend. ZSS veroorzaakt een verstoring van het evenwicht waardoor de waterdiepte groter wordt. Bij constante snelheid van ZSS ontwikkelt de diepte op den duur naar een dynamische evenwichtswaarde als de ZSS snelheid onder een kritische limiet blijft. De dynamische evenwichtsdiepte neemt niet-lineair toe met de toenemende ZSS snelheid, en gaat naar oneindig groot (verdrinking) als de kritische ZSS snelheid wordt benaderd. Boven de kritische ZSS snelheid is er dus geen eindig dynamische evenwichtsdiepte te definiëren. De kritische ZSS snelheid is gelijk aan de evenwichtsdiepte (zonder ZSS) gedeeld door een tijdschaal. Verrassend is dat deze tijdschaal niet gelijk aan de morfologische tijdschaal t.o.v. het morfologische evenwicht is, maar gelijk aan de morfologische tijdschaal maal de macht in de

modelformulering voor evenwichtssedimentconcentratie. Dit betekent dat het type sediment invloed heeft op de kritische ZSS snelheid. Voor systemen met dezelfde evenwichtsdiepte en dezelfde morfologische tijdschaal is de kritische ZSS snelheid groter voor de systemen met fijner sediment. Uit de analyse is ook geconcludeerd dat het tijdproces voor het bereiken van het dynamische evenwicht sterk afhangt van de snelheid van ZSS. De morfologische tijdschaal t.o.v. het dynamische evenwicht neemt niet-lineair toe met de ZSS snelheid, het wordt oneindig groot als de ZSS snelheid de kritische limit voor verdrinking nadert. Het niet-lineaire gedrag van het dynamische evenwicht en de bijbehorende morfologische tijdschaal heeft als gevolg dat de respons van een bekken op ZSS van relatieve hoge snelheid dezelfde lijkt ongeacht of de snelheid (niet ver) onder, gelijk of boven de kritische limiet is. De verschillende zeegatsystemen in de Waddenzee kunnen heel verschillend reageren op ZSS (van dezelfde snelheid) omdat de respons van een systeem wordt bepaald door de verhouding tussen de ZSS snelheid en de kritische snelheid.
Voordat de modellen zijn aangepast op basis van de nieuwste inzichten uit de data analyse zijn de vier toekomstige ZSS scenario's gesimuleerd met de bestaande modellen. Evaluatie van de modelresultaten voor de periode tot heden dient als basis voor de aanpassing van de modellen. Het model voor Eierlandse Gat is aangepast om het sedimenttransport door de zeegat van een import naar export te veranderen. Dit is bereikt door de getijslag groter te maken en het lineair te laten toenemen in de tijd. De modelresultaten blijken gevoelig te zijn voor de lineaire trend van de getijslag. De modellen voor Vlie en Marsdiep zijn aangepast om de huidige import door Marsdiep te verlagen en die door Vlie te vergroten. Dit is bereikt door de morfologische evenwichtstoestanden in de bekkens te veranderen.

Voor beide systemen is het evenwichtsvolume van de platen zodanig aangepast dat de evenwichtshoogte van de platen (met het voorgeschreven plaatareaal dat tijdens de simulatie niet verandert) 40% van de getijslag wordt, conform de empirische relatie. Verder is het evenwichtsvolume van de geulen in Marsdiep verhoogd. De veranderingen hebben als gevolg dat het sedimenttekort in het bekken van Marsdiep kleiner en die van het Vlie groter wordt. Met de aangepaste modellen zijn de vier ZSS scenario's opnieuw gesimuleerd. De modelresultaten zijn geëvalueerd en vergeleken met die van de simulaties vóór de modelaanpassing. De resultaten van de modellen, zowel vóór als na de aanpassingen, leiden tot een aantal dezelfde conclusies (zie Figuur hieronder):

- Er is een vertraging in de respons van de zeegatsystemen op de verandering van ZSS. De vertraging is groter voor de zeegaten met grotere bekkens, en die met een sedimenttekort in de bekkens door ingrepen in het verleden. De verschillen in ZSS tussen de scenario's beginnen in 2020, maar de verschillen in sedimenttransport door de zeegaten worden pas merkbaar in 2030 voor Pinkegat en Eierlandse Gat, en pas aan het eind van de eeuw voor Marsdiep.

Title
Sediment exchange between the Wadden Sea and North Sea Coast

Client	Project	Attribute	Pages
Rijkswaterstaat Water, Verkeer en Leefomgeving, UTRECHT	1220339-008	1220339-008-ZKS-0006	53

- De verschillen in de sedimentimport naar de Waddenzee tussen de verschillende scenario's zijn relatief klein. De ZSS snelheid in 2100 verschilt een factor 4 tussen de scenario's, maar de berekende totale sedimentimport naar de Waddenzee tussen de hoogste (ongeveer 7.5 miljoen m3 per jaar) en de laagste (ongeveer 5 miljoen m3 per jaar) scenario's is ongeveer 2.5 miljoen m^3 per jaar in 2100. Tot 2060 zijn de verschillen niet significant.
- De veranderingen van de sedimentimport in de toekomst t.o.v. de huidige situatie zijn niet erg groot. Voor alle scenario's neemt de totale sedimentimport eerst af in de tijd door het dempen van de verstoringen door de ingrepen in het verleden. De versnelling van ZSS buigt deze afnemende trend om, maar niet vóór 2050 in alle beschouwde scenario's. Voor de hoogste ZSS scenario (8 mm/j) zal de import ongeveer 1.5 miljoen m^3 per jaar toenemen in 2100 t.o.v. de huidige situatie (ongeveer 6 miljoen m3 per jaar).

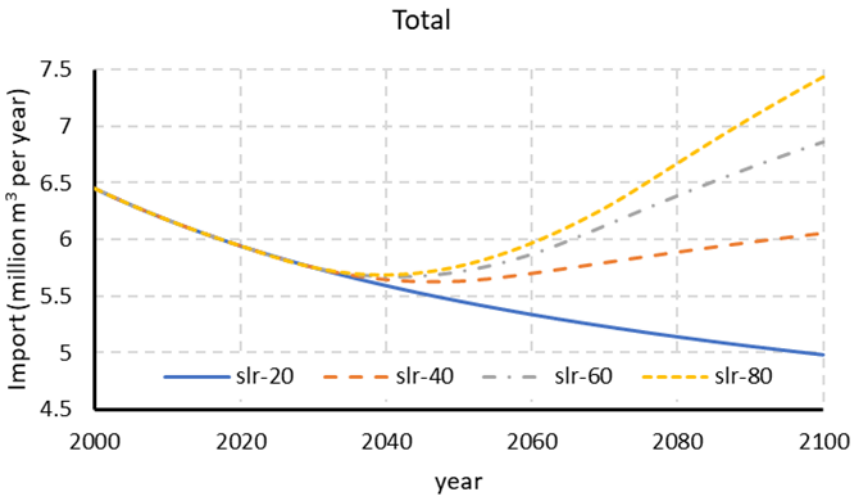

Berekende totaal sedimenttransport naar de NL Waddenzee door de zeegaten

Deze conclusies moeten gecombineerd worden met de resultaten van de data-analyse studies om een volledig en kwantitatief beeld te krijgen in de ontwikkelingen van de sedimentuitwisselingen door de verschillende zeegaten. Het bepalen van de huidige sediment behoefte kan het best worden gebaseerd op de resultaten van de sedimentbalans analyse op basis van bodemhoogtegegevens (Elias, 2019). De combinatie van de waarden voor de huidige import naar de Waddenzee en de conclusies uit de huidige studie geeft een volledig beeld voor de toekomstige ontwikkelingen van de import. Verder zijn de volgende aanbevelingen gedaan:

- Onderzoek naar suppletiestrategieën die sedimentimport naar de Waddenzee kan beïnvloeden.
- Combineer veldwaarnemingen met modellering voor monitoring naar effecten van (veranderende) ZSS.
- Meer aandacht besteden aan de studies via data analyse en procesmodellering om de sedimentuitwisseling door de zeegaten beter te begrijpen en te bepalen.

Deltares

Title
Sediment exchange between the Wadden Sea and North Sea Coast

Client	Project	Attribute	Pages
Rijkswaterstaat Water, Verkeer en Leefomgeving, UTRECHT	1220339-008	1220339-008-ZKS-0006	53

- Onderzoek naar veranderingen van getijslag t.g.v. morfologische veranderingen in de zeegatsystemen.
- Uitbreiding van de huidige ASMITA modelleringsstudie door ook de ontwikkelingen van de verschillende morfologische elementen te beschouwen.
- De verschillende verbeteringen van het ASMITA model, zoals al zijn voorgesteld in literatuur, implementeren: gegradeerde sedimenttransport module, uitbreiden met een morfologisch element kwelder, betere parameter-setting aan de hand van procesmodellering.

Contents

1 Introduction **1**
1.1 Background / problem 1
1.2 Objectives 1
1.3 Approach 2
1.4 Outline of the report 3

2 ASMITA modelling for the Dutch Wadden Sea **5**
2.1 Introduction 5
2.2 Model formulation 5
2.2.1 Aggregation of the convection-diffusion equations for suspended sediment concentration 5
2.2.2 Exchange between bottom and water column 7
2.2.3 ASMITA formulation 10
2.3 On parameter settings 15
2.4 Dutch Wadden Sea applications 17
2.5 Possible improvements and limitations 18

3 Theoretical analysis **21**
3.1 A single element model for a tidal basin 21
3.2 Dynamic equilibrium and critical SLR rate 21
3.3 Transient development 24
3.4 Concluding discussions 26

4 Simulating sediment exhanges **29**
4.1 Sea-level rise scenarios 29
4.2 Existing parameter setting 31
4.3 Improvement of the models 37
4.3.1 Eierlandse Gat Inlet 37
4.3.2 Texel Inlet and Vlie 38
4.3.3 Results updated runs 41

5 Concluding discussions **45**
5.1 Updating of the ASMITA models 45
5.2 Model results 46
5.3 Uncertainties 47
5.4 Relevance for management 48
5.5 Recommendations 49

6 References **51**

1 Introduction

1.1 Background / problem

Sediment exchange between the (North Sea) coastal zone and the Wadden Sea is important for various management and policy aspects. For coastal maintenance related to long-term flood protection it is important because the exchange is an important item in the sediment budget of the coastal foundation. The nourishment requirement along the coast is thus partly determined by this exchange. It is important for the Wadden Sea because the growth of the intertidal flats of high ecological values with sea level rise (SLR) depends on this sediment exchange. Insight into the sediment exchanges between the coastal zone and the Wadden Sea through the various tidal inlets is essential for the management of the Dutch coastal system. That is the reason why gaining / improving this insight is an important objective for various research programs such as Kustgenese 2, B&O Kust, KPP Wadden Sea etc.

Data analysis is an important method to gain insight into the sediment exchange between the coastal zone and the Wadden Sea. The sediment budget for the Wadden Sea area based on the analysis of the bathymetric data not only directly provides the exchanges through the inlets in the past, but also provides insight into the morphological status of the Wadden Sea (Elias et al., 2012; Wang et al., 2018). For example, we know that exchanges are not only determined by SLR but are also influenced to a large extent by human interventions in the past.

This large influence of human interference not only makes it difficult to understand the present-day and even past behaviour of the Wadden Sea, but also makes predictions of its future state challenging. Through detailed analysis of data and detailed modelling of the physical processes (such as done in the framework of Kustgenese 2 and SEAWAD) we can start to understand and unravel the present-day processes. These insights can be summarized in conceptual models that can help us better understand its future behaviour. Extrapolating present-day trends and knowledge provides a direct prediction of the near future trends in which we can probably safely assume that processes remain the same. Such assumption is not valid on the longer-term timescales. On these longer timescales (decades to centuries) SLR will start to become increasingly important for the sediment exchange processes. This is especially true for the inlets that are already close to equilibrium (e.g. the eastern Wadden Sea). Here the future sediment losses to the basin will be determined by demand of the basin. In the Western Wadden Sea, the effect of SLR is more difficult to predict and understand. At present the system is still far from equilibrium and we do not fully know when or how the effects of SLR will start to dominate the sediment exchanges. Nevertheless, by making certain assumptions and running scenarios we can still learn and gain insight in the effect of various SLR scenarios on future sediment exchanges.

1.2 Objectives

The aim of the present study is to predict the long-term developments of sediment exchanges through the tidal inlets between the Dutch Wadden Sea and the (North Sea) coastal zone. Results from the study will be used for the technical advice from the Kustgenese 2 research program.

The study will focus on the following research questions:

- What will be the differences in sediment exchange rates through the tidal inlets connecting the Dutch Wadden Sea and the coastal zone between future (up to 2100) and present?
- What will be the influences of the different sea-level scenarios on the future sediment exchange rates?

1.3 Approach

To make predictions of the sediment exchange through the Wadden Sea inlets we can use

1 Data analysis (e.g. sediment budgets).
2 Process-based modelling (e.g. Delft3D).
3 Aggregate modelling (e.g. ASMITA).

Data Analysis. Extensive sediment-budget analyses based on primarily the Vaklodingen datasets have already been carried out (Elias et al., 2012; Wang et al., 2018; Elias, 2018; 2019). For this study, it is important that the relevant insights from the previous analyses are properly implemented (especially with respect to the morphological equilibrium) in the aggregated modelling.

Process-based modelling. Various Delft3D models for the Dutch Wadden Sea are available. These models are not directly suitable for performing long-term morphodynamic simulations that can predict long-term sediment exchange on the scale of the entire Wadden Sea. These models have not been designed or validated for this task, and performing the model simulations would result in unfeasible long run times and computational expense. However, the models are suitable for improving our detailed understanding of the processes and mechanisms underlying the sediment exchange, and for determining the correct model parameter settings for aggregated modelling.

Aggregate modelling. The ASMITA model was developed to simulate the long-term large-scale morphological developments of tidal inlet systems (Stive et al., 1998; Stive and Wang, 2003). The sediment exchange through the inlet is a direct output of the model. If properly set up and calibrated, this model is therefore ideally suited for achieving the objective of this study.

ASMITA model schematisation for each tidal inlet system in the Dutch Wadden Sea already exist. These models have been used to simulate developments under the influence of SLR (Van Goor et al., 2003). However, the models were developed and set up about 20 years ago, and various suggestions for improvements have since then been made. An extensive inventory of this has been provided by Townend et al. (2016a, b). It is currently not well known how these improvements would influence the answers to the questions asked here. More important is the fact that ASMITA uses the relationships for the morphological equilibrium. These relationships must be adjusted based to represent the latest insights from recent data analysis studies (Wang et al. 2018; Elias, 2018, 2019). The ASMITA models for the various tidal inlets will therefore first be adapted, at least with respect to the morphological equilibrium. The other improvements to the models according to the suggestions in the literature will not be implemented for the time being. The models will not be calibrated in detail using the latest data, but we will look closely at the latest results from the data analysis concerning sediment transport through the tidal inlets for adjusting the models. The simulations are then performed for four different SLR scenarios.

A theoretical analysis based on a simplified ASMITA model can help us to link ASMITA modelling to the analysis of historical observations and process modelling. More importantly for the present study, the insights from the analysis are also helpful for the interpretation of the ASMITA model results.

1.4 Outline of the report

Chapter 2 provides the background information on the model concept of ASMITA. This chapter intents to clarify the possibilities and restrictions of the models. This also provides the appropriate background to correctly analyse the results and draw conclusions. In Chapter 3 a theoretical analysis is carried out in order to get insights how tidal basins like those in the Wadden Sea respond to changing SLR. The insights from the analysis are useful for the interpretation of the model results presented in Chapter 4. In Chapter 5 conclusions from the study are summarised and recommendations are given.

2 ASMITA modelling for the Dutch Wadden Sea

2.1 Introduction

ASMITA (Aggregated Scale Morphological Interaction between Tidal basin and Adjacent coast) was first proposed by Stive et al. (1998) for modelling long-term morphological development of tidal inlet systems in the Wadden Sea. In this chapter background information of the model concept is provided (2.2), overviews of the research on the parameter settings (2.3) and applications of the model to the Wadden Sea (2.4) are given. An overview of possible model improvements is summarised in Section. 2.5. All this information is meant to give insights in the possibilities and restrictions of the used models, to provide an essential background for the correct interpretation of the model results.

2.2 Model formulation

2.2.1 Aggregation of the convection-diffusion equations for suspended sediment concentration

First we explain how the equations for sediment concentration at different levels of aggregation in space and time are related to each other (see also Townend et al., 2016a).

We start with the 3D convection-diffusion equation governing the sediment concentration:

$$\frac{\partial c}{\partial t}+\frac{\partial uc}{\partial x}+\frac{\partial vc}{\partial y}+\frac{\partial wc}{\partial z}-\frac{\partial}{\partial x}\left(\varepsilon_x\frac{\partial c}{\partial x}\right)-\frac{\partial}{\partial y}\left(\varepsilon_y\frac{\partial c}{\partial y}\right)=w_s\frac{\partial c}{\partial z}+\frac{\partial}{\partial z}\left(\varepsilon_z\frac{\partial c}{\partial z}\right) \tag{2-1}$$

Herein

c	=	sediment concentration [-],
t	=	Time [T],
u, v	=	horizontal flow velocity components [LT^{-1}],
x, y	=	horizontal coordinates [L],
w	=	vertical flow velocity [LT^{-1}],
z	=	vertical coordinate [L],
$\varepsilon_x, \varepsilon_y, \varepsilon_z$	=	turbulent diffusion coefficients in x-, y- and z-direction [L^2T^{-1}],
w_s	=	settling velocity of sediment particles [LT^{-1}].

This is in fact the mass-conservation equation for sediment, forming the kinetic part of the theory for suspended sediment transport. The dynamic part of the theory for suspended sediment transport is in the bed boundary condition. At the boundary near the bed the sediment concentration or the sediment concentration gradient can be prescribed. Their values need to be calculated using a sediment transport formula (in the case of sand) or a formulation for the erosion rate (in the case of mud).

Equation (2-1) can be integrated in the vertical direction to obtain the depth-averaged advection-diffusion equation:

$$\frac{\partial h\overline{c}}{\partial t}+\frac{\partial \alpha_x \overline{u} h\overline{c}}{\partial x}+\frac{\partial \alpha_y \overline{v} h\overline{c}}{\partial y}-\frac{\partial}{\partial x}\left(D_x h\frac{\partial \overline{c}}{\partial x}\right)-\frac{\partial}{\partial y}\left(D_y h\frac{\partial \overline{c}}{\partial y}\right)=f_b \qquad (2\text{-}2)$$

With the over-bar representing depth-averaging of the corresponding variable, and

- h = water depth [L],
- α_x, α_y = coefficients counting for the effects of the shapes of the vertical distribution of flow velocity and sediment concentration [-],
- D_x, D_y = dispersion coefficients [L^2T^{-1}],
- f_b = sediment exchange flux between the bed and the water column [LT^{-1}].

This can be considered as the first level of aggregation as used by many process-based models. Note that the diffusion coefficients in the horizontal direction become dispersion coefficients as they also represent the mixing due to the non-uniform vertical distributions of the flow velocity and the sediment concentration.

For non-cohesive sediment (sand) the sediment exchange between the bottom and the water column can be derived using an asymptotic solution of the convection-diffusion equation (2-1) (Gallappatti and Vreugdenhil, 1985; Wang, 1992). For cohesive sediment (mud) these terms can be calculated using e.g. the Krone-Partheniades formulation (see Winterwerp and van Kesteren, 2004). In both cases f_b consists of two parts, an erosion part depending on the flow conditions and sediment properties and a deposition part proportional to the sediment concentration.

The next level of aggregation can be carried out by integrating equation (2-2) over the width of a river, estuary or a channel:

$$\frac{\partial A\overline{c}}{\partial t}+\frac{\partial \alpha \overline{u} A\overline{c}}{\partial x}-\frac{\partial}{\partial x}\left(AD_x\frac{\partial \overline{c}}{\partial x}\right)=F_b \qquad (2\text{-}3)$$

With the over-bar now representing averaging over the cross-section, and

- A = cross-sectional area [L^2],
- α = coefficients counting for the effects of the distribution of flow velocity and sediment concentration within the cross-section [-],
- D_x = dispersion coefficients [L^2T^{-1}],
- F_b = sediment exchange flux between the bed and the water column, f_b integrated over the width [L^2T^{-1}].

This is the equation for suspended sediment concentration used in 1D-network models.

Equation (2-2) can also be written as

$$\frac{\partial h\overline{c}}{\partial t}+\frac{\partial s_x}{\partial x}+\frac{\partial s_y}{\partial y}=f_b \qquad (2\text{-}4)$$

In which s_x and s_y represent the suspended sediment transport rate [L^2T^{-1}] in x- and y-direction. This equation can further be aggregated by integrating over a part, or the whole, of an estuary or a tidal basin (a morphological element). Using Green's theorem, the integration yields:

$$\frac{\partial VC}{\partial t} = \sum_i S_i + F_B \tag{2-5}$$

Herein

- V = volume of the water body of the area [L^3],
- S_i = sediment transport at open boundary (positive=directed to the element, i.e. import) [L^3T^{-1}],
- C = averaged sediment concentration in the element,
- F_B = Sediment exchange flux between the bed and the water column, i.e. f_b integrated over the element.

This equation can also be directly derived by considering the mass-balance of sediment in the whole water body.

Equations (2-2), (2-3), (2-4) and (2-5) can also be aggregated in time, e.g. over a tidal period or a much longer time. As an example, integration of Eq. (2-3) over a tidal period yields:

$$\frac{\partial u_r h\overline{c}}{\partial x} + \frac{\partial v_r h\overline{c}}{\partial y} - \frac{\partial}{\partial x}\left(D_x h \frac{\partial \overline{c}}{\partial x} \right) - \frac{\partial}{\partial y}\left(D_y h \frac{\partial \overline{c}}{\partial y} \right) = f_b \tag{2-6}$$

The first term representing the change of sediment storage in the water column is neglected as it becomes much less important on longer timescale than the terms on the right hand side representing the exchange with the bottom. All the other terms remain basically the same, but the parameters and variables now represent the tidally-averaged values. The residual flow velocities (u_r, v_r) causes advection and the tidal flow now becomes the major mixing agent for the dispersion represented by the coefficients D_x and D_y [L^2T^{-1}], as elaborated by Wang et al. (2008).

Aggregation in time of Eq. (2-5) yields the equation used by ASMITA.

$$\sum_i S_i + F_B = 0 \tag{2-7}$$

2.2.2 Exchange between bottom and water column

The advection-diffusion equation itself, no matter its level of aggregation, describes mass-balance for suspended sediment. It does not describe any dynamics but only the kinetics of suspended sediment transport, because the equation itself does not provide the information on the flux of sediment exchange between the bottom and the water column. In its aggregated forms (Eqs. 2-2 through 2-7) this flux is a term in the equation itself and can thus not be determined by solving the equation but needs to be prescribed. In fact, this flux determines the morphological change as well and its formulation represents the dynamic part of the suspended sediment transport model.

For the 3D form (Eq. 2-1) this dynamic part is introduced via the bed boundary condition. At the boundary near the bed the sediment concentration, the vertical gradient of the sediment concentration or a linear combination of the two can be prescribed. In case of prescribing the sediment concentration it is often argued that the concentration close near the bed can instantaneously adjust to the local flow condition and therefore the equilibrium value of the concentration can be prescribed. In fact, the argument other way around should be used: For steady uniform flow the solution for the sediment concentration vertical far away from the boundary is the equilibrium concentration profile. The prescribed value at the bed boundary is therefore per definition the equilibrium concentration. The similar arguments can be made for the prescribed concentration gradient at the bed. Physically, by prescribing the concentration the vertical flux due to settling is given but the vertical flux due to turbulent mixing is left free, and by prescribing the concentration gradient the opposite is true. For non-cohesive sediment the required equilibrium concentration or equilibrium concentration gradient depends on the flow conditions and the sediment properties and can be determined with one of the many sediment transport formulas (e.g. van Rijn, 1993). Note that the equilibrium values of concentration and its gradient are related to each other as at equilibrium the downwards settling flux and the upwards flux due to turbulent mixing balance each other. For cohesive sediment deposition and erosion rates according to the Krone-Partheniades formulation is often used for the bed boundary condition. According to this formulation deposition only occurs when bed shear stress τ is below a critical value τ_d and erosion only occurs if bed shear stress is above another critical value τ_e. With this formulation it is not always possible to define the instantaneous equilibrium concentration by balancing the deposition and erosion rates. For $\tau_d<\tau_e$ this leads to an equilibrium concentration equal to zero for $\tau<\tau_d$, undetermined for $\tau_d<\tau<\tau_e$ and infinitely large if $\tau>\tau_e$. However, if the hydrodynamic condition is fluctuating due to e.g. tide, a tide-averaged equilibrium concentration can often be well defined.

The advection-diffusion equations only aggregated in space but not aggregated in time (Eqs. 2-2 & 2-3) are also used in process-based models. The flux f_b or F_b can be calculated with the Krone-Partheniandes formulation for cohesive sediment or with a formulation derived from an asymptotic solution of the (3D) advection-diffusion equation (Gallappatti and Vreugdenhil, 1985; Wang, 1992) for none-cohesive sediment. These formulations require information concerning hydrodynamic conditions expressed in flow velocity, bed shear stress, etc. in addition to the sediment properties e.g. D_{50}:

$$f_b = F\left(\bar{u}, \tau, D_{50}, \ldots\right) \tag{2-8}$$

Due to the aggregation in time the required detailed information on hydrodynamic condition, as required by a sediment transport formula or the Krone-Partheniades formulation, is no longer available. The sediment exchange flux between the bottom and the water column needs then to be expressed in the available aggregated morphological and hydrodynamic parameters. This formulation, representing the dynamics of sediment, is dependent on the level of aggregation and makes the difference between the various models. The formulations have often the form

$$f_b = \gamma w_s \left(c_e - c\right) \tag{2-9}$$

Herein w_s is the settling velocity [LT^{-1}], γ is a dimensionless coefficient, c is sediment concentration and c_e is the equilibrium value of c. This is similar as the formulation of Gallappatti and Vreugdenhil (1985) for process-based models. The differences between the models are in the way of calculating c_e.

Di Silvio (1989) relate the equilibrium concentration to the morphological state variable. As an example, for shoals influenced by wind waves he uses

$$c_e \propto h^{-n} \tag{2-10}$$

in which h is the water depth and n is a power. It is noted that this relation implicitly defines the morphological equilibrium at which $c=c_e$ is equal to the sediment concentration prescribed at the open boundary of the model.

In the ESTMORF (Wang et al., 1998) and ASMITA (Stive et al., 1998) models the equilibrium concentration is dependent on the ratio between the morphological state variable and its equilibrium value. As an example, for the channels in ESTMORF the formulation is:

$$c_e = c_E \left(\frac{A_e}{A} \right)^n \tag{2-11}$$

Herein A is the cross-sectional area of the channel with A_e as its equilibrium value, c_E is a coefficient which can be considered as the global equilibrium concentration because when the whole system is in morphological equilibrium $c=c_e=c_E$ applies. The rationale behind this formulation is that the ratio A_e/A is actually an indicator for the flow strength in the channel with respect to the equilibrium situation, as A_e increases with increasing tidal prism. The formulation is thus analogous to a power law for sediment transport capacity.

It now becomes clear that the essential difference between aggregated and so-called process-based models (e.g. ASMITA and Delft3D) is the level of aggregation rather than the degree in which their formulations contain empirical elements. They both use the advection-diffusion equation for the suspended sediment transport. The formulations concerning sediment dynamics, i.e. the exchange between bed and water column, contain empirical elements in both models. ASMITA makes use of the empirical relations for morphological equilibrium and Delft3D uses a sediment transport formula which is also empirical in character. The empirical elements in both models also involve the same degree of uncertainties. In this sense, it is not meaningful to classify the two types of models as respectively (semi-)empirical and process-based.

In addition to the aggregation level and the formulation for the sediment exchange flux between bed and water column, the hydrodynamic module helps to differentiate the various models. Obviously, the implemented hydrodynamic module depends to a large extent on the aggregation level of the model. As an example, the models ESTMORF (Wang et al., 1998) and ASMITA (Stive et al., 1998) are based on the same type of formulations. However, ESTMORF can be coupled to a full (process-based) 1D network hydrodynamic model to simulate the required aggregated hydrodynamic parameters of tidal volume and tidal range, whereas, due to the higher level of aggregation, ASMITA calculates the tidal prism for the prescribed tidal range and plane area. Process-based models can be 1D, 2DH or 3D depending on the hydrodynamic module used.

2.2.3 ASMITA formulation

Schematisation

ASMITA has a high level of spatial aggregation. A tidal inlet system is schematised into a limited number of morphological elements, at a level similar to that of the ebb-tidal delta as described by (Walton and Adams, 1976). For each element a water volume below a certain reference level or a sediment volume above a certain reference plane (not necessarily horizontal) acts as the state variable. A tidal inlet is typically schematised into the following three elements (Fig.2.1):

- The ebb-tidal delta, with its state variable V_d = total excess sediment volume relative to an undisturbed coastal bed profile [L^3],
- The inter-tidal flat area in the tidal basin, with its state variable V_f = total sediment volume between MLW and MHW [L^3],
- The channel area in the tidal basin, with its state variable V_c = total water volume below MLW [L^3].

The adjacent coastal areas, which can exchange sediment with the inlet system, are considered as an open boundary, ‘the external world’.

Although commonly used for a tidal inlet system, this 3-elements-schematisation is not the only possible schematisation. In fact, an ASMITA model can contain any number of inter-connected morphological elements. A necessary requirement is that the morphological equilibrium of each element is defined and can be evaluated from the available (aggregated) hydrodynamic parameters in the model. In the following, this 3-element schematisation is used to explain the model formulation and to demonstrate some applications. In addition, a 1-element model is used to explain certain points, in which the whole back barrier basin of the tidal inlet is considered as a single morphological element with the state variable water volume V in the basin below MHW [L^3].

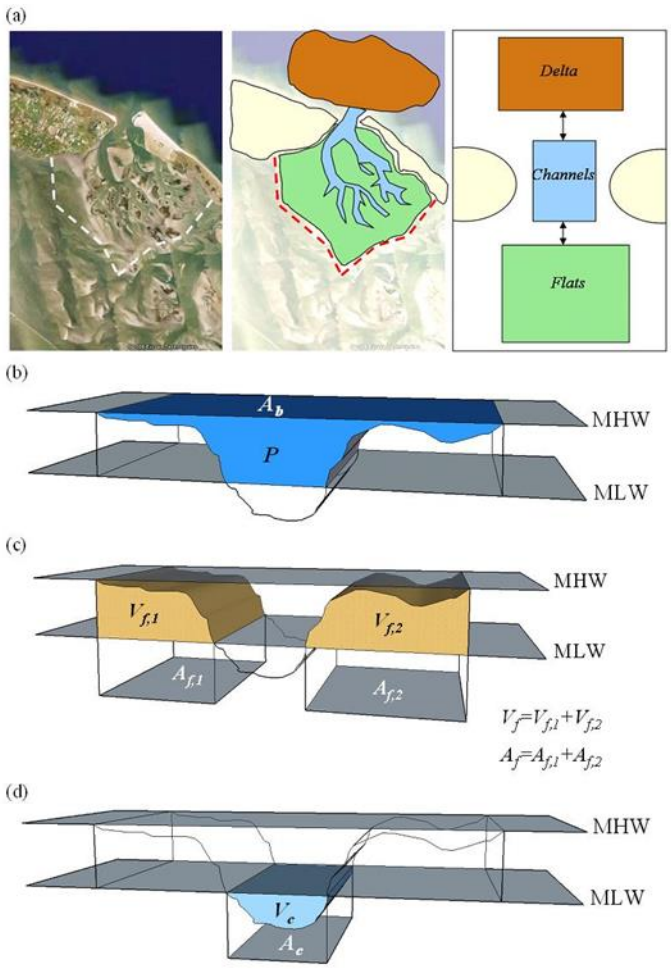

Figure 2.1 The 3 elements schematisation for a tidal inlet in ASMITA and the definitions of the hydrodynamic and morphological parameters basin area A_b *and tidal prism* P *(b), area* A_f *and volume* V_f *of tidal flats (c), area* A_c *and volume* V_c *of channels (d).*

Hydrodynamics

If the morphology of a tidal inlet system is only defined by the volumes of the three morphological elements mentioned above (see also Figure 2.1) it does not need to model the hydrodynamics in detail. In fact, only the tidal range in the back-barrier basin and the tidal prism are needed to define the morphological equilibrium state. Tidal basins, such as those in the Wadden Sea, are relatively small in size with respect to the tidal wave length. For such short basins it is acceptable to use the water volume between high and low water for the tidal prism. When the intertidal volume is defined in terms of sediment volume, the relation between the tidal amplitude a and the tidal prism P is given by:

$$P = 2A_b a - V_f \tag{2-12}$$

Herein A_b is the horizontal area of the basin at MHW. The tidal range in the basin is dependent on the tidal range in the open sea as well as dependent on the morphological state of the tidal inlet system. The tidal range in the open sea should be considered as a boundary condition. It is difficult to model the influence of the morphological changes on the tidal range due to the

highly aggregated schematisation. However, for short basins like those in the Wadden Sea, the influence of the morphological changes on the tidal range is limited. Therefore, the tidal amplitude in the basin *a* is prescribed. It is noted that it is still possible to have *H* varying in time, to take account of any trend or a cyclic change e.g. the nodal tide variation (Jeuken et al., 2003; Wang and Townend, 2012). It is also noted that the model does take into account of the feedback from the morphological development to the hydrodynamics, via Eq. (2-12), because V_f is a morphological state variable.

Morphological equilibrium state

For all three elements, empirical relationships are required to define their morphological equilibrium dimensions. With these relationships the morphological equilibrium state of a tidal basin is fully determined if the basin area A_b and the tidal amplitude a are given. The equilibrium relationships can be prescribed in various ways (see Townend et al, 2016). Here we outline the approach that has been used to study the dynamics of the Wadden Sea.

For the intertidal flat there are two empirical relationships used, one for its area and one for its height (Renger and Partenscky, 1974, Eysink and Biegel, 1992).

$$\frac{A_{fe}}{A_b} = 1 - 2.5 \cdot 10^{-5} \sqrt{A_b} \tag{2-13}$$

$$h_{fe} = 2\alpha_{fe} a \tag{2-14}$$

Herein A_{fe} [m^2] is the equilibrium tidal flat surface area; A_b [m^2] is basin surface area; a is tidal amplitude and according to Eysink (1990)

$$\alpha_{fe} = \alpha_f - 0.24 \cdot 10^{-9} A_b \tag{2-15}$$

with α_f = 0.41. The equilibrium volume of the intertidal flat, i.e. the sediment volume between low water (MLW) and high water (MHW), is thus by definition:

$$V_{fe} = A_{fe} h_{fe} \tag{2-16}$$

The channel volume V_c is defined as the water volume under MLW in the basin. Its equilibrium value is related to the tidal prism as follows:

$$V_{ce} = \alpha_c P^{1.55} \tag{2-17}$$

The equilibrium volume of the ebb tidal delta is also related to the tidal prism (Walton and Adams, 1976)

$$V_{de} = \alpha_d P^{1.23} \tag{2-18}$$

Using these equations with various empirical coefficients (the α's) the morphological equilibrium of a tidal basin can be determined from two parameters, the total basin area A_b and the tidal amplitude a. For a single element model for the back-barrier basin the total water volume of the basin below MHW, which is the sum of the channel volume (below LW) V_c and the tidal prism, can be used (see further Chapter 3):

$$V = V_c + P = F\left(A_b, a\right) \tag{2-19}$$

Sediment transport and morphological change

As explained in the previous section, the sediment transport processes are described by the mass-balance equation for sediment for each of the element aggregated in time (Eq.2-7). Following the schematisation shown in Fig.2.1 these equations are:

for flats

$$S_{cf} + F_{Bf} = 0 \tag{2-20}$$

for channels

$$S_{dc} - S_{cf} + F_{Bc} = 0 \tag{2-21}$$

for the ebb-tidal delta

$$S_{od} - S_{dc} + F_{Bd} = 0 \tag{2-22}$$

In these equations S is the sediment transport, and its subscripts indicate from which element to which element (f = flat, c = channel, d = ebb tidal delta, o = outside world). S_{cf} is thus the sediment transport from the element channel to the element flat. Because of the aggregation in time, the transports are governed by the diffusion / dispersion with the tidal flow as mixing agent (the advection term vanished as no river inflow is considered):

$$S_{cf} = \delta_{cf}\left(c_c - c_f\right) \tag{2-23}$$
$$S_{dc} = \delta_{dc}\left(c_d - c_c\right) \tag{2-24}$$
$$S_{od} = \delta_{od}\left(c_o - c_d\right) \tag{2-25}$$

In these equations c is suspended sediment concentration, and its subscript indicates the morphological element. δ is the horizontal exchange coefficient with the dimension [L^3T^{-1}] and depends on the dispersion coefficient, the area of the cross-section connecting the two elements and the distance between the two elements (see Wang et al., 2008). Its subscripts have the same meaning as those of S.

F_B is the sediment exchange flux between bed and water column representing erosion minus sedimentation. Its second subscript again indicates the morphological element. Similar to Eq. (2-9) they are formulated as follows:

$$F_{Bf} = w_f A_f\left(c_{fe} - c_f\right) \tag{2-26}$$
$$F_{Bc} = w_c A_c\left(c_{ce} - c_c\right) \tag{2-27}$$
$$F_{Bd} = w_d A_d\left(c_{de} - c_d\right) \tag{2-28}$$

In these equations A is the horizontal area [L^2] of the element and w is the vertical exchange velocity [LT^{-1}], which is proportional to the settling velocity of sediment (see Eq. 2-9). Their subscripts indicate the element. Note that the vertical exchange velocity is not necessarily the same for all three elements even if only a single fraction of sediment is present. As discussed earlier, the equilibrium sediment concentrations are calculated by comparing the morphological state with its equilibrium for each of the elements:

$$c_{fe} = C_f \left(\frac{V_f}{V_{fe}} \right)^{n_f} \tag{2-29}$$

$$c_{ce} = C_c \left(\frac{V_{ce}}{V_c} \right)^{n_c} \tag{2-30}$$

$$c_{de} = C_d \left(\frac{V_d}{V_{de}} \right)^{n_d} \tag{2-31}$$

In these equations, the coefficients C have the dimension of sediment concentration and n is a power similar to that in a power-law sediment transport formula (Wang et al., 2008). Note the difference in the formulations between the elements flat and delta with a sediment volume as morphological state variable and the channel element with water volume as state variable (sediment volume relationships are the inverse of the water volume relationship).

The sediment exchange between bed and water (Eqs. 2-25 thought 2-27) also determines the change of the morphological state variable of the corresponding element:

$$\frac{\mathrm{d}V_f}{\mathrm{d}t} = -F_{Bf} = -w_f A_f \left(c_{fe} - c_f \right) \tag{2-32}$$

$$\frac{\mathrm{d}V_c}{\mathrm{d}t} = F_{Bc} = w_c A_c \left(c_{ce} - c_c \right) \tag{2-33}$$

$$\frac{\mathrm{d}V_d}{\mathrm{d}t} = -F_{Bd} = -w_d A_d \left(c_{de} - c_d \right) \tag{2-34}$$

If all morphological elements in the whole system are in equilibrium, F_B should vanish for all elements, thus the sediment concentration is equal to its equilibrium value for each of the elements ($c_f=c_{fe}$, $c_c=c_{ce}$,. $c_d=c_{de}$). The equations (2-20) - (2-22) yield: $S_{cf}=S_{dc}=S_{od}=0$, i.e. all residual sediment transports vanish, and it follows then from equations (2-23)-(2-25) that $c_f=c_c=c_d=c_o$, and thus also $c_{fe}=c_{ce}=c_{de}$. According to equations (2-29) - (2-31) $c_{fe}=C_f$, $c_{ce}=C_c$, $c_{de}=C_d$ if all the elements are in equilibrium (their volumes equal to their equilibrium values). Now it follows $C_f=C_c=C_d=c_o$. Thus, the coefficients in equations (2-29) - (2-31) should be the same and all equal to the sediment concentration at the open boundary (the outside world). This constant is called the global equilibrium concentration C_E:

$$C_f = C_c = C_d = c_o = C_E \tag{2-35}$$

Any deviation from this rule implies a redefinition of the morphological equilibrium state.

2.3 On parameter settings

The physical parameters in an aggregated model (ASMITA or ESTMORF) can be divided into two groups: parameters that define the morphological equilibrium state and parameters that determine the morphological timescales.

The former group contains all the coefficients in the empirical relations for the morphological equilibrium state. To determine these coefficients, we have to rely on the field data and little use can be made of experience gained elsewhere. The latter group of coefficients, determining the morphological timescales, includes the overall equilibrium sediment concentration c_E, the power n in the formulation for the local equilibrium concentration, the vertical exchange coefficient w_s, and the horizontal inter-tidal dispersion coefficient D (in ESTMORF) or the horizontal exchange coefficient δ (L^3T^{-1}) (in ASMITA). Note that the following relation between the two parameters applies:

$$\delta = \frac{DA}{L} \tag{2-36}$$

Herein A is the cross-sectional area [L^2] linking the two elements in ASMITA and L is the distance [L] between the two elements.

These parameters are not directly measurable. However, as made clear in the previous section, the essential difference between an aggregated model (e.g. ASMITA) and a process-based model (e.g. Delft3D) is the level of aggregation and not the considered physical processes. Therefore, the parameters in the two types of models must be related to each other. Based on a theoretical analysis, the following conclusions concerning the model parameters influencing the morphological timescales in the aggregated models ESTMORF and ASMITA haven been drawn by Wang et al. (2008):

- The power n in the formulation of the local equilibrium sediment concentration should be equal to the velocity exponent in the power law sediment transport formula.
- The overall equilibrium sediment concentration c_E is a parameter indicating the level of morphological activity in the area. From a calibration point of view, it has the same function as the coefficient of proportionality in the sediment transport formula in a process-based morphodynamic model.
- The vertical exchange coefficient w should be proportional to and of the same order of magnitude as the settling velocity of the sediment particles.
- The inter-tidal dispersion coefficient D should be proportional to u^2H/w in which u is scale of the tidal flow velocity and H is the water depth. This can also be written as

$$\frac{D}{uH} \propto \frac{u}{w} \tag{2-37}$$

By evaluating the existing applications of ESTMORF it has further been concluded that (Wang et al., 2008):

- The product nc_E determines the order of magnitude of the morphological timescale. In a calibration procedure, these two parameters can only be separated if the field data available concern a situation beyond the application domain of the linear model, i.e. far from morphological equilibrium.

- As long as Equation (2-37) is satisfied, the mixing by the tidal flow is correctly represented by the inter-tidal dispersion formulation. The parameters w_s and D can only be separated in a calibration procedure if the field data available encompass a sufficiently wide range of spatial scales in the morphological changes. Especially the smaller-scale changes are essential.
- The field data used to calibrate the existing applications of ESTMORF did not cover a sufficiently wide range to allow the model parameters to be separated. As long as the calibrated models are applied to problems in the same range of morphological change, this should not be of relevance.

Based on these conclusions it is recommended that the results from the theoretical analysis are used to inform the process of model calibration. The following calibration procedure is recommended:

- Chose the value of n based on an applicable sediment transport formula.
- Chose w based on the settling velocity of the sediment particles.
- Chose D based on Equation (2-37) and the experience gained from the existing applications, i.e.

$$\frac{D}{uH} = \varepsilon \frac{u}{w} \tag{2-38}$$

  with ε in the order of 0.1 (final value to be chosen during calibration). Here the tidal flow velocity scale is assumed to be of the order of 1 m/s.

- Adjust c_E to give the correct morphological timescale.

In this way the number of the calibration parameters reduces to 2, viz. ε and c_E.

The ASMITA models for the Wadden Sea tidal inlet systems were set up and calibrated before these rules for the parameter setting were derived. The parameters determined from the calibration, in e.g. the model used by Van Goor et al. (2003) for analysing the effect of SLR, do not fully satisfy these rules. Wang et al. (2014) revisited the modelling of Van Goor et al. (2003) by first recalibrating the model following the rules presented above. With the new parameter setting, the calculated critical SLR rate for drowning of the tidal flats became unrealistically low. This agrees with the modelling results of Dissanayake et al. (2012) using Delft3D. The theoretically derived rules thus indeed make the two types of models agree with each other, but the results concerning critical SLR rate become worse instead of improved. The reason for the unrealistic results is due to the fact that both models only consider a single sand fraction, whereas in reality mud also plays a rule in the morphological development of the Wadden Sea. By taking into account the contribution of mud to grow of the tidal flats the results of Van Goor et al. (2003) can be reproduced again (Wang and Van der Spek, 2015). It is thus concluded that the parameters derived from the model calibration accounts for the effects of sand as well as mud transport although a single fraction sediment transport model is used. If the theoretically derived rules for the parameter setting in aggregated models are followed then at least two sediment fractions (sand and mud) need to be considered. For the process-based models this means that sand as well as mud needs to be taken into account for modelling e.g. the response of tidal inlet systems to SLR. Hofstede et al. (2018) showed that process-based modelling of the impact of SLR on the Wadden Sea can indeed be more successful if sand as well as mud is considered in the model (see also Becherer et al., 2018).

The implementation of mud transport in ASMITA by Wang and Van der Spek (2015) is very simple and meant for demonstrating the importance of mud for the Wadden Sea in responding to accelerated SLR. This implementation is not used in this study.

2.4 Dutch Wadden Sea applications

The development of ASMITA started in end 1990's. The model was first applied for studying the effects of land subsidence within the framework of the first Environmental Impact Assessment study for gas extraction under the Wadden Sea (Eysink et al., 1998; Buijsman, 1997). In this application a tidal inlet system is schematised into five elements, tidal flat in the basin, channel in the basin, ebb-tidal delta, and two adjacent coast elements (one on each side of the ebb-tidal delta). The two coast elements exchange sediment with the outside world.

Later, for each of the tidal inlets in the Dutch Wadden Sea (Texel Inlet, Eierlandse Gat, Vlie, Ameland Inlet, Pinkegat and Zoutkamperlaag, see Figure 2.2) an ASMITA model has been set up. These application models were set up in the Msc. projects of Van Goor (2001) and Kragtwijk (2001), of which the major results are published in Van Goor et al. (2003) and Kragtwijk et al. (2004). A tidal inlet system was then schematised into three morphological elements: tidal flats in the basin, channels in the basin and the ebb-tidal delta. The two coast elements in the schematisation of Buijsman (1997) are removed and considered as outside world. Van Goor et al. (2003) studied the effect of SLR on Eierlandse Gat Inlet and Ameland Inlet using an ASMITA model. The same schematisation was used for setting up ASMITA models for the other inlet systems in the Dutch Wadden Sea (Kragtwijk et al., 2004; Bijsterbosch, 2003; Hinkel et al., 2013).

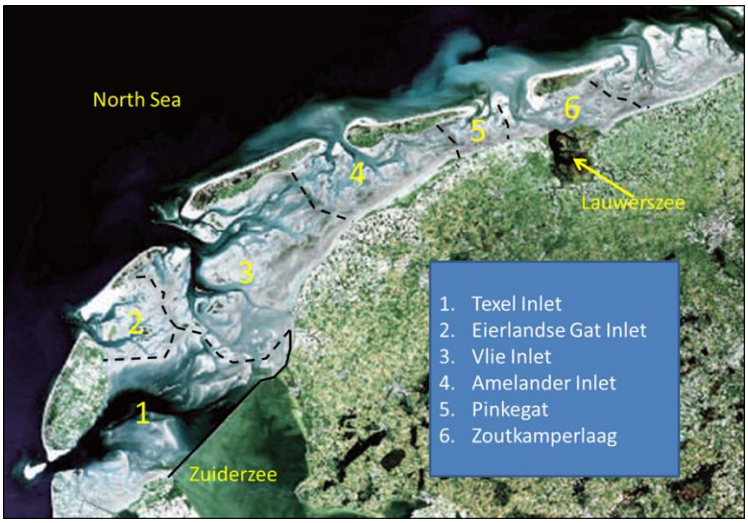

Figure 2.2 Tidal basins in the Dutch Wadden Sea

The schematisation and parameter settings reported in Kragtwijk (2001) have been used in various studies later, in which the parameter settings have been adjusted. Wang and Eysink (2005) used the models for Pinkegat and Zoutkamperlaag in the second EIA study for gas extraction under Wadden Sea. Wang et al. (2006) implemented the ASMITA models for the tidal inlets in the PONTOS-ASMITA model for the NL Coast. In this study the parameter setting in the model for Texel Inlet has been adjusted following the insight from Elias (2006) that the sediment import through this inlet had been much higher than until then was thought and the system was still far from dynamic equilibrium due to the closure of the Zuiderzee.

The parameter settings reported by Wang et al. (2006) are considered as most up to date, despite of a number of attempts of further improvements of the models (Van Geer, 2007; Wang et al., 2007; Wang and van der Spek, 2015). Wang et al. (2018) used these parameter settings to calculate the critical rates of SLR (R_c) for drowning of the tidal flats in the tidal inlet systems following the formulation of Van Goor et al. (2003; see also Bijsterbosch, 2003; Hinkel et al., 2013), see Table 2.1 Parameter settings for the ASMITA model and critical sea-level rise rates for the tidal basins in the Dutch Wadden Sea..

Table 2.1 Parameter settings for the ASMITA model and critical sea-level rise rates for the tidal basins in the Dutch Wadden Sea.

Inlet	Texel	Eierland	Vlie	Ameland	Pinkegat	Zoutkamp
C_E (-)	0.0002	0.0002	0.0002	0.0002	0.0002	0.0002
w_{sf} (m/s)	0.0001	0.0001	0.0001	0.0001	0.0001	0.0001
A_f (km^2)	133	105	328	178	38.1	65
A_c (km^2)	522	52.7	387	98.3	11.5	40
A_d (km^2)	92.53	37.8	106	74.7	34	78
δ_{od} (m^3/s)	1550	1500	1770	1500	1060	1060
δ_{dc} (m^3/s)	2450	1500	2560	1500	1290	1290
δ_{cf} (m^3/s)	980	1000	1300	1000	840	840
R_c (mm/yr)	**7.0**	**18.0**	**6.3**	**10.4**	**32.7**	**17.1**

2.5 Possible improvements and limitations

An extensive inventory of the possible improvements for the existing ASMITA models is given by Townend et al. (2016a, b). All the improvements on software level are not implemented for the simulations in this study. It is then important to know the shortcomings of the used models for the correct interpretation of the model results. Every shortcoming of the models corresponds to some uncertainties of the model results.

For each of the tidal inlet a separate ASMITA model is set up. This means that the tidal divides in the Wadden Sea are considered as fixed and closed boundaries between the back-barrier basins of the tidal inlets. In reality, the tidal divides are not closed for water flow, nor for sediment transport. This simplification / shortcoming of the ASMITA model schematisations is one of the reasons why the parameters in the empirical relations for the morphological equilibrium are system specific rather than constant for all systems and why they need to be adjusted following the insights from the data analysis studies each time (see Chapter 4).

The horizontal areas of the three morphological elements in the ASMITA model for a tidal inlet system are fixed and thus do not change in time. This means that the effects of the movements of the tidal divides in the Wadden Sea are not taken into account. The change in the distribution between channels and tidal flats, i.e. between subtidal and intertidal parts, within a tidal basin due to morphological changes cannot be taken into account either.

Due to the high level of aggregation, the hydrodynamic module in the used models is reduced to a relation between the tidal prism and the tidal range. However, effect of morphological changes on these two parameters is only taken into account via the relation between the tidal prism and the tidal flat volume. The effects on the development of the tidal range (and the corresponding effect on the tidal prism) cannot be taken into account, and needs to be prescribed for the simulations.

In the used ASMITA models a single fraction sediment transport module is used. In reality, sand as well as mud are important for the morphological development of the Wadden Sea. The relevance of making distinction between sand and mud for modelling the effects of SLR for tidal basins has been discussed by Wang and Van der Spek (2015), but a robust version of ASMITA with a multi-fraction sediment transport module implemented is not yet available.

3 Theoretical analysis

3.1 A single element model for a tidal basin

For the theoretical analysis we adopt a single element model for tidal basins with the water volume below HW V as state variable. Following the definitions (see Fig.2.1), we have

$$V = V_c + P \tag{3-1}$$

As the tidal basins are relatively small compared to the tidal wave length, the tidal prism *P* can be calculated as

$$P = 2A_b a - V_f \tag{3-2}$$

Herein A_b is the basin area and *a* is the tidal amplitude. As the equilibrium values of V_c and V_f can be calculated from a and P, the equilibrium value of V is thus a function of *a* and A_b:

$$V_e = F\left(A_b, a\right) \tag{3-3}$$

The single element ASMITA model yields (see Stive and Wang, 2003):

$$\frac{dV}{dt} = \frac{w\delta c_E A_b}{\delta + wA_b}\left[\left(\frac{V_e(t)}{V(t)}\right)^n - 1\right] + A_b R \tag{3-4}$$

Herein

t	=	Time
w	=	Vertical exchange coefficient,
δ	=	Horizontal exchange coefficient,
n	=	Power in the formulation for the local equilibrium concentration,
c_E	=	Overall equilibrium concentration,
R	=	Relative sea-level rise rate

3.2 Dynamic equilibrium and critical SLR rate

Equation (3-4) has already been used in earlier studies to demonstrate that there is a critical limit R_c of sea-level rise rate beyond which the tidal basin will be drown (see Stive and Wang, 2003; van Goor et al., 2003; Wang et al., 2018):

$$R_c = \frac{w\delta c_E}{\delta + wA_b} \tag{3-5}$$

Equation (3-4) can be also be written in terms of depth

$$\frac{dH}{dt} = \frac{w\delta c_E}{\delta + wA_b}\left[\left(\frac{H_e(t)}{H(t)}\right)^n - 1\right] + R \tag{3-6}$$

With

$$H = \frac{V}{A_b} \quad \text{and} \quad H_e = \frac{V_e}{A_b} \tag{3-7}$$

The equations can be made dimensionless using

$$h = \frac{H}{H_e} = \frac{V}{V_e} \tag{3-8}$$

And

$$\tau = \frac{t}{T} \qquad \text{with} \qquad T = \frac{V_e}{A_b w c_E} + \frac{V_e}{\delta c_E} = \frac{H_e}{w c_E} + \frac{A_b H_e}{\delta c_E} \tag{3-9}$$

Yielding

$$\frac{dh}{d\tau} = \left[\left(\frac{1}{h}\right)^n - 1\right] + r \tag{3-10}$$

Herein

$$r = \frac{R}{R_c} \tag{3-11}$$

It is noted that using Equations (3-5) and (3-9) the critical sea-level rise rate can be written as

$$R_c = \frac{H_e}{T} \tag{3-12}$$

It should also be noted that T is not equal to the morphological timescale T_m as defined by linearizing Equation (3-4) or Equation (3-6) for the case R=0 (see Kragtwijk et al., 2004). The relation between the two timescales is

$$T = nT_m \tag{3-13}$$

These relations reveal several interesting things worth knowing:

- Equation (3-12) for R_c reveals the importance of the timescale *T.* In this relation H_e, the equilibrium depth, can be determined more easily. Empirical relations are available from which its value can be evaluated if the tidal range $2a$ and the size of the tidal basin is known, H_e=F(A_b, a). Moreover, it can also be connected to direct

observations. For basins which are more or less in equilibrium, as e.g. because it has not been impacted by human interference for a long time, the equilibrium depth can be evaluated from the measured bathymetry. Note that a correction is necessary when it is in a dynamic equilibrium as it has been forced by sea-level rise with a constant rate for a long time (See Fig.3.1). An example within the Dutch Wadden Sea is the Ameland Inlet.

- Equation (3-12) can also be used for estimating the timescale T if R_c can be derived from observations. This is e.g. the case for the Texel Inlet, in which a large sediment deficit arose after the closure of the Zuiderzee in 1932 (Elias, 2012; Wang et al., 2018). The system can practically be considered as 'drowned' because of this large sediment deficit, implying that the observed sedimentation rate is close to the critical sea-level rise rate.
- The power n influences the morphological timescale, but not the critical sea-level rise rate. It does influence the dynamic equilibrium state as well (as elaborated below).

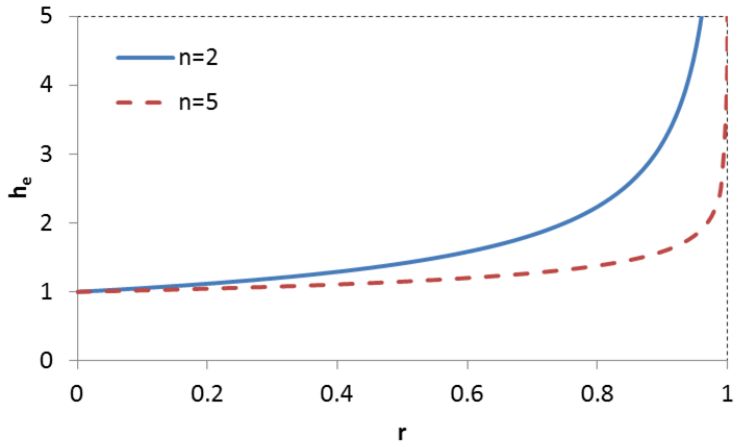

Figure 3.1 Influence of the power n *on the dynamic morphological equilibrium*

In dimensionless form the dynamic equilibrium morphological state can be derived from Eq. (3-7):

$$h_e = (1-r)^{-\frac{1}{n}} \tag{3-14}$$

This relation is shown in Figure 3.1 which clearly indicates that the dynamic equilibrium morphological state is sensitive to the value of n. The larger the n value, the smaller the h_e value for the same dimensionless sea-level rise rate r. This means that for larger n values, the deviation of the dynamic equilibrium from the morphological equilibrium according to the empirical relations is smaller. Fig.3.1 also shows that for larger n values, the transition from gradual increase to rapid increase of h_e occurred at a larger value of r. However, the magnitude of n has also influence on the critical SLR according to Eq. (3-12) and (3-13): the larger the n value, the lower the critical rate for the same morphological timescale.

3.3 Transient development

It is also important to know about the time process of the development towards the new dynamic equilibrium when SLR accelerates. Some insight into this process can already be obtained from the morphological timescale, determined by linearizing Eq. (3-10) at $h=h_e$ (i.e. at the dynamic morphological equilibrium):

$$\tau_a = \frac{1}{n\left(1-r\right)^{\frac{n+1}{n}}} \tag{3-15}$$

τ_a is the dimensionless time (value of τ) after which a deviation from the dynamic equilibrium would be decreased with a factor e according to the linearized model. For r=0, τ_a=1/n which is the same relation between the morphological timescale and the timescale T as given by Eq. (3-13), implying that a larger n results into a smaller morphological timescale for the same value of T. The morphological timescale depends on the SLR rate r, the larger the r vale, the larger the morphological timescale. This means that for a higher accelerated SLR rate it takes longer time before the new dynamic morphological equilibrium is reached.

Figure 3.2 shows the results of the non-linear model (solution of Eq. (3-10)) for various combinations of n and r. For all the simulations shown in this figure $h(0)$=1 is used as initial condition, i.e. starting at equilibrium for r=0. The influence of the magnitudes of n and r on the transient development, as indicated by the morphological timescale described above, agrees qualitatively well with the results of the non-linear model.

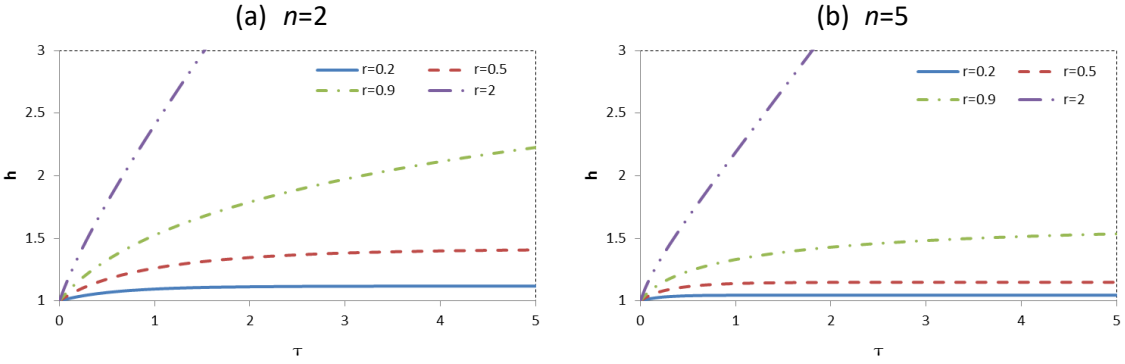

Figure 3.2 Transient development for various SLR rates starting from equilibrium state (h(0)=1). Influence of the power n can be seen by comparing the two panels, (a) for n=2 and (b) for n=5.

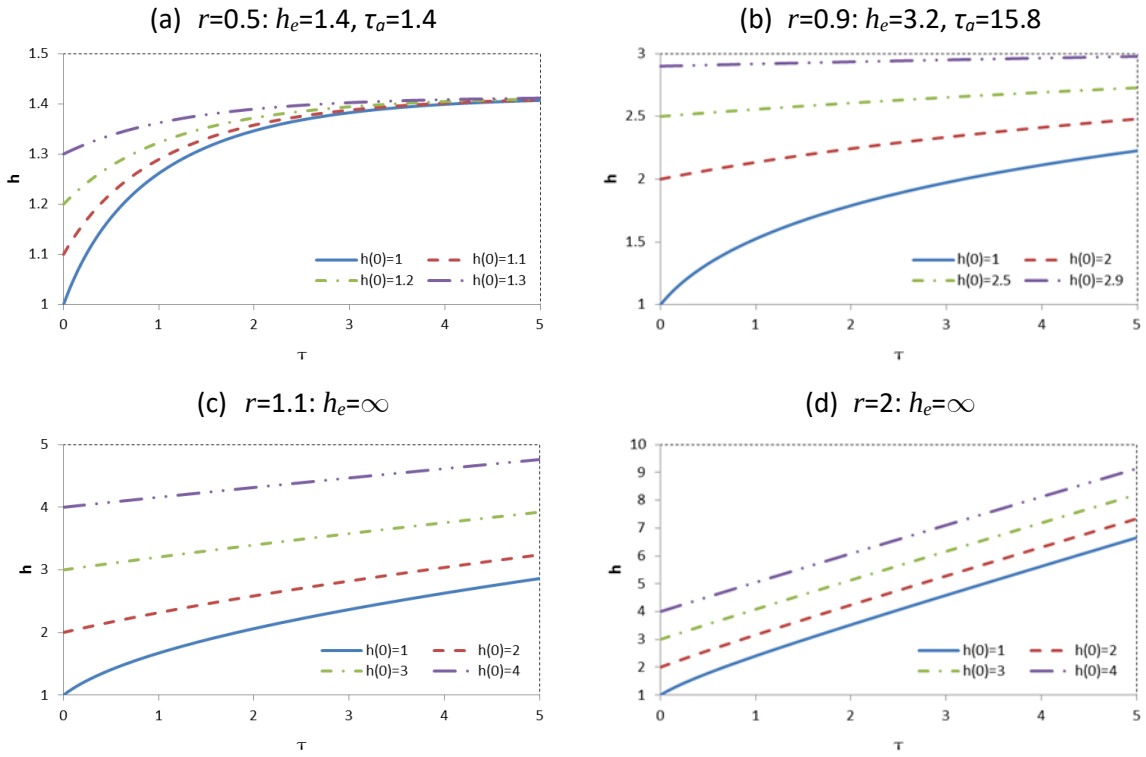

Figure 3.3 Transient development starting from various initial conditions for four SLR rates: (a) r=0.5 (SLR far below critical rate), (b) r=0.9 (SLR just below critical rate), (c) r=1.1 (SLR just above critical rate), (d) r=2 (SLR far above critical rate), in all cases n=2. The dynamic equilibrium h_e and the morphological timescale τ_a are given in the title of the panels.

Acceleration of SLR starts not likely at a moment that the tidal basins are in equilibrium (h=1). Therefore, the influence of the initial condition is investigated for four SLR rates (Figure 3.3), two below and two above the critical rate. For the two cases with SLR rate below the critical rate, a finite dynamic equilibrium depth exists. The dynamic equilibrium is being achieved in all simulations for both cases. The difference between the two cases concerns not only the dynamic equilibrium, but especially the morphological timescale. For SLR rate equal to half the critical rate (r=0.5) the dimensionless morphological timescale is about 1.4 and it increases to about 15.8, i.e. more than 10 times larger if the SLR rate is equal to 90% of the critical value (r=0.9). When the SLR rate approaches the critical value the morphological timescale increases to a very large value (Figure 3.4). For the two cases with the critical SLR rate exceeded, no dynamic equilibrium can be defined, and the water depth increases to infinitely large. The behavior of the development is not much influenced by the initial depth. Especially for the case that the SLR rate is far above the critical rate (Fig.4d) all the lines are parallel. This is due to the fact that h increases fast to a large value, and when h is large the right-hand side of Eq. (3-10) becomes nearly constant. Physically this means that there is a maximum rate of sediment transport to the basin, which is achieved when the water depth in the basin becomes large, implying that further change of the depth has little influence on the sediment transport rate.

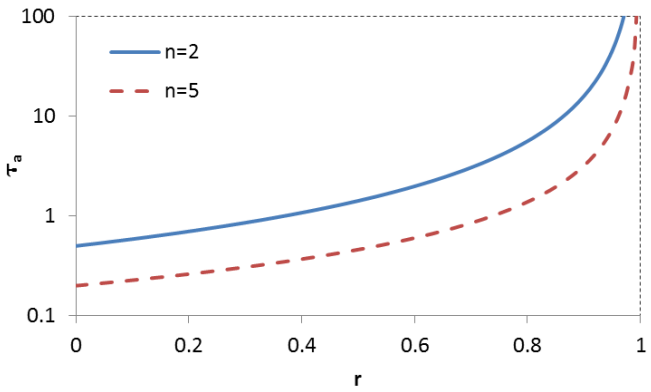

Figure 3.4 Morphological timescale as function of sea-level rise rate

3.4 Concluding discussions

In summary, two findings from the theoretical analysis are new and can be considered as important insights in the response of tidal basins to SLR:

1. The critical SLR rate can be determined from the morphological equilibrium and the morphological timescale (with respect to morphological equilibrium).
2. The morphological timescale with respect to the dynamic morphological equilibrium is strongly influenced by the SLR rate.

These two findings and their implications are more elaborated in the following.

Ad1. Combination of Equations (3-12) and (3-13) yields $R_c=H_e/nT_m$. This relation can be used for estimating the critical SLR rate from observations. Because of the very large timescale involved it is practically impossible to determine R_c directly from observations. However, the equilibrium depth can be determined from the field observations of relatively limited period, directly or indirectly via empirical relations. The morphological timescale T_m can also be derived from observed development if the considered system is disturbed from its equilibrium. The influence of the power *n* according to this relation implies that the type of sediment is important. A sandy system can behave very differently than a muddy system. This explains also the findings by Wang and Van der Spek (2015): After increasing the *n* value from 2 to 5 the critical SLR rate became much lower even though the model was calibrated to have the same morphological timescale in both cases.

Ad2. It is essential to realize that it is the morphological timescale with respect to the dynamic morphological equilibrium that determines how long it take before the new dynamic morphological equilibrium is achieved when SLR accelerates. This morphological timescale is different than the one with respect to the morphological equilibrium (for R=0). It needs to be determined by linearizing the model with respect to the dynamic morphological equilibrium. This morphological timescale increases with increasing SLR rate non-linearly (Fig.3.4). It increases to infinity as SLR rate approaches the critical value. Physically this can be explained by the delayed response of the tidal basin to acceleration of SLR and the limitation of sediment transport capacity through the inlet. The delayed response has the consequence that the effect of acceleration in SLR on sediment exchange between the basin and the coastal area will only be noticeable after a long time. The limitation of sediment transport capacity implies that even on the long term the sediment import to the basin cannot increase proportionally to SLR rate.

For the tidal basin itself it means that acceleration of SLR will cause loss of tidal flat area, and the total loss will only be achieved after a long time.

The non-linear behavior of the system concerning dynamic morphological equilibrium and the corresponding morphological timescale implies that a tidal basin responds to a relatively high SLR rate in the same way, no matter if the SLR rate is below, equal or above the critical rate. It will thus be very difficult if not impossible to determine the critical rate of SLR by monitoring.

4 Simulating sediment exhanges

4.1 Sea-level rise scenarios

Four scenarios of SLR will be considered in the present study, one without and three with acceleration:

1. Continuation of the present SLR rate: *R* is constant and equal to 2 mm/y;
2. R=2 mm/y until 2020, and R=4 mm/y in 2100;
3. R=2 mm/y until 2020, and R=6 mm/y in 2100;
4. R=2 mm/y until 2020, and R=8 mm/y in 2100.

For the exact way how the sea-level rises in the three accelerating scenarios reference is made to the position paper of Wadden Academy (Vermeersen et al., 2018). Vermeersen presented three scenarios, see Figure 4.1. According to these scenario's the SLR rates in 2100 are respectively about 5, 7 and 12 mm/y. Further analysis on the variation of the SLR scenarios learned that in the three scenarios the SLR rate increases linearly in time until a maximum is reached (end of acceleration period). The rate of increase is higher, and the period of acceleration is longer for a higher scenario. The acceleration ends in 2030, 2060 and 2100 respectively for the three scenarios.

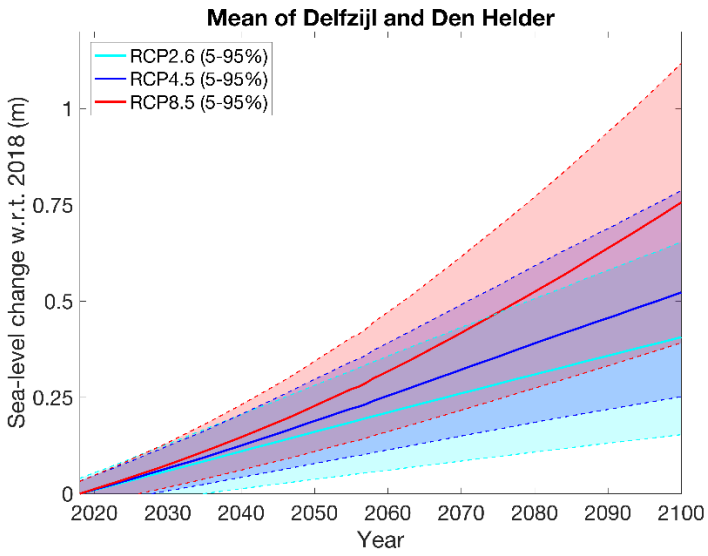

Figure 4.1 Sea-level rise scenarios presented in Vermeersen et al. (2018).

It is further noted that in the scenarios of Vermeersen et al. (2018) the acceleration of SLR started earlier than 2020, in contradiction of the scenarios defined here. Based on these considerations the four scenarios in the present study are exactly defined as follows (see Figure 4.2).

1. Continuation of the present SLR rate: R is constant and equal to 2 mm/y;
2. R=2 mm/y until 2020, from 2020 to 2050 R increases linearly to 4 mm/y, and then remain constant, R=4 mm/y;
3. R=2 mm/y until 2020, from 2020 to 2060 R increases linearly to 6 mm/y, and then remain constant, R=6 mm/y;
4. R=2 mm/y until 2020, from 2020 to 2070 R increases linearly to 8 mm/y, and then remain constant, R=8 mm/y.

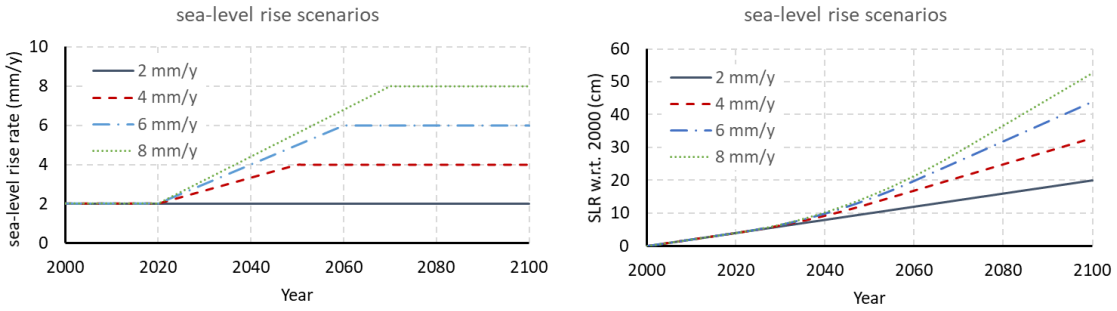

Figure 4.2 The four sea-level rise scenarios considered in the present study. Left: change of SLR rate; right: SLR since 2000.

4.2 Existing parameter setting

First, the four SLR scenarios are simulated with the ASMITA models with the existing (latest) parameter setting (see Wang et al., 2006). All the input parameters are given in Table 4.1. It is noted that for the tidal flat the equilibrium volume is specified instead of α_f in the empirical relation (2-15). This does not induce extra restrictions to the model because according to the empirical relations (2-13) and (2-14) the equilibrium volume of tidal flat is fully determined for given basin area and tidal range. This is also more practical because in the present version of the model the horizontal areas of the morphological elements including the tidal flat are fixed during the simulation.

Table 4.1 Input parameters of the ASMITA application models for the tidal inlets (symbols explained in chapter 2)

Inlet	Texel	Eierland	Vlie	Ameland	Pinkegat	Zoutkamp
Basic configuration: tidal range and the horizontal areas of the three elements						
2a (m)	1.65	1.65	1.90	2.15	2.15	2.25
A_f (km^2)	133	105	328	178	38.1	65
A_c (km^2)	522	52.7	387	98.3	11.5	40
A_d (km^2)	92.53	37.8	106	74.7	34	78
Parameters influencing morphological timescale						
n (-)	2	2	2	2	2	2
C_E (-)	0.0002	0.0002	0.0002	0.0002	0.0002	0.0002
w_{sf}(m/s)	0.0001	0.0001	0.0001	0.0001	0.0001	0.0001
w_{sc} (m/s)	0.0001	0.00005	0.0001	0.00005	0.0001	0.0001
w_{sd} (m/s)	0.00001	0.00001	0.00001	0.00001	0.00001	0.00001
δ_{od} (m^3/s)	1550	1500	1770	1500	1060	1060
δ_{dc} (m^3/s)	2450	1500	2560	1500	1290	1290
δ_{cf} (m^3/s)	980	1000	1300	1000	840	840
Initial conditions: volumes of the three morphological elements in 1970						
V_{f0} (Mm^3)	51.5	55	162	120	29.6	69
V_{c0} (Mm^3)	2160	106	1230	302	18.5	177
V_{d0} (Mm^3)	509.1	132	369.7	131	35	151
Parameters for defining the morphological equilibrium						
V_{fe} (Mm^3)	151	57.83	190	131.2	30.3	70
α_c (10^{-6})	10	13.13	9.6	10.241	10.14	27.266
α_d (10^{-3})	4.025	8	2.662	2.92157	6.9278	9.137

The simulated sediment import into the tidal basins (i.e. transport from the ebb-tidal delta to channel in the basin) are depicted in Figure 4.3.

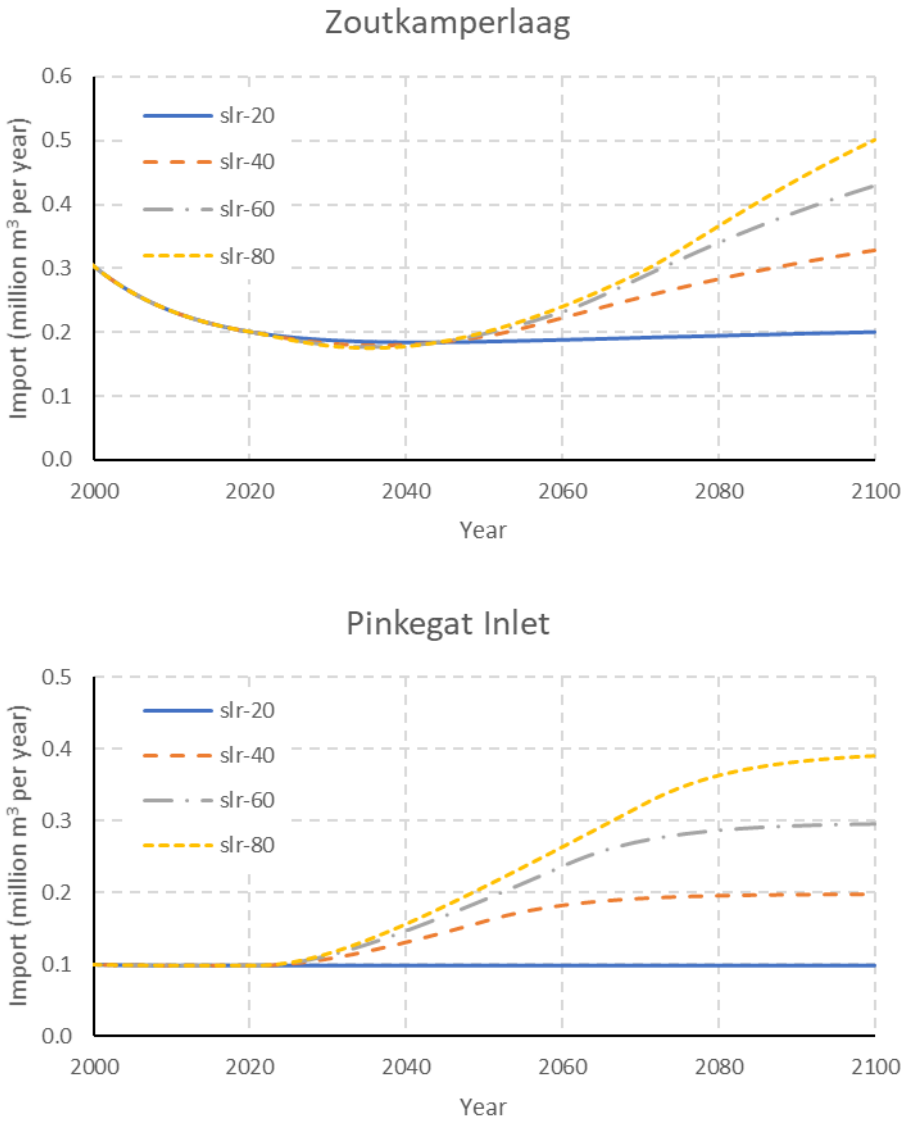

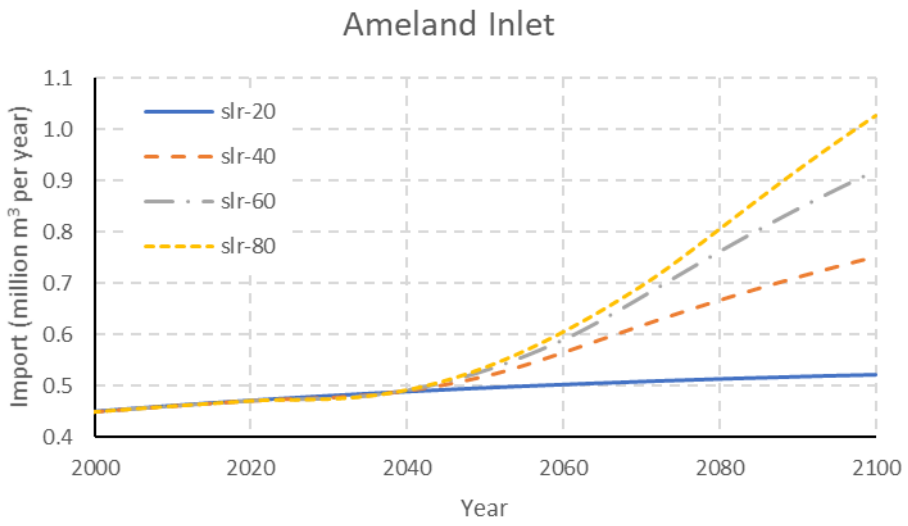
Ameland Inlet
Import (million m3 per year)
1.1
1.0
0.9
0.8
0.7
0.6
0.5
0.4
slr-20
slr-40
slr-60
slr-80
2000
2020
2040
2060
2080
2100
Year

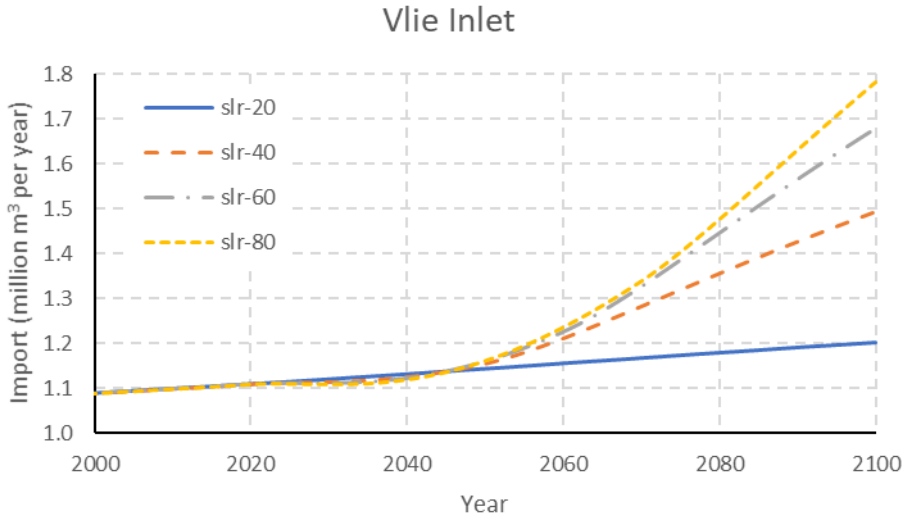
Vlie Inlet
Import (million m3 per year)
1.8
1.7
1.6
1.5
1.4
1.3
1.2
1.1
1.0
slr-20
slr-40
slr-60
slr-80
2000
2020
2040
2060
2080
2100
Year

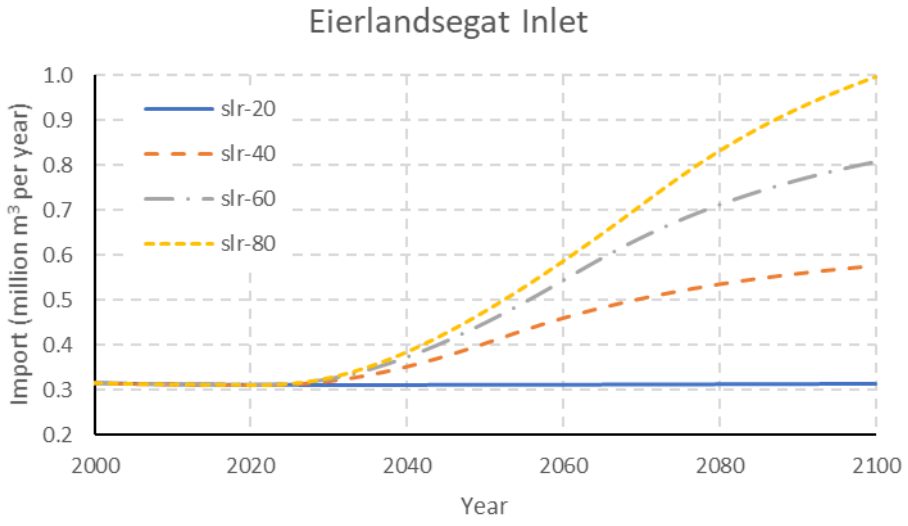
Eierlandsegat Inlet
Import (million m3 per year)
1.0
0.9
0.8
0.7
0.6
0.5
0.4
0.3
0.2
slr-20
slr-40
slr-60
slr-80
2000
2020
2040
2060
2080
2100
Year

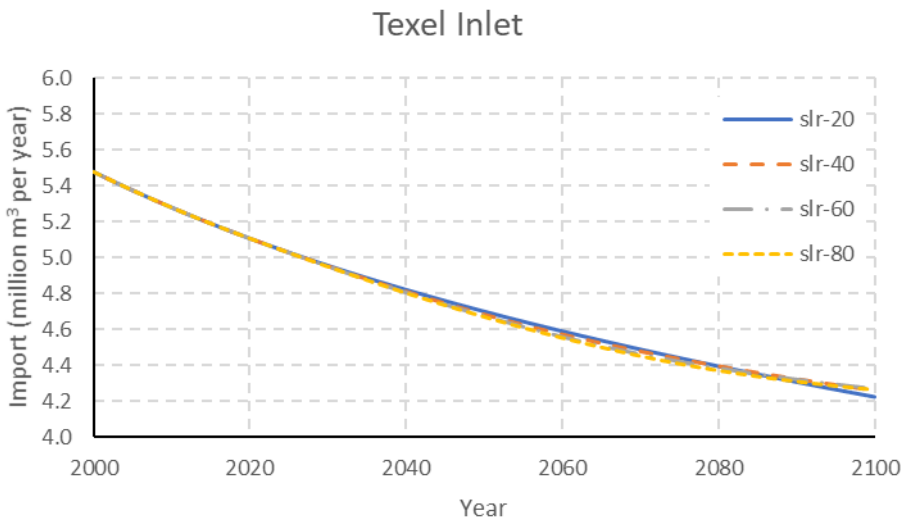

Figure 4.3 Sediment transport exchange between the Wadden Sea basins and the North Sea coasts through the various tidal inlets (positive = directed to Wadden Sea).

In Figure 4.4 the total import to the western part (Texel, Vlie and Eierlandsegat inlets), eastern part (Ameland, Pinkegat, and Zoutkamperlaag inlets) and the total Dutch Wadden Sea are presented.

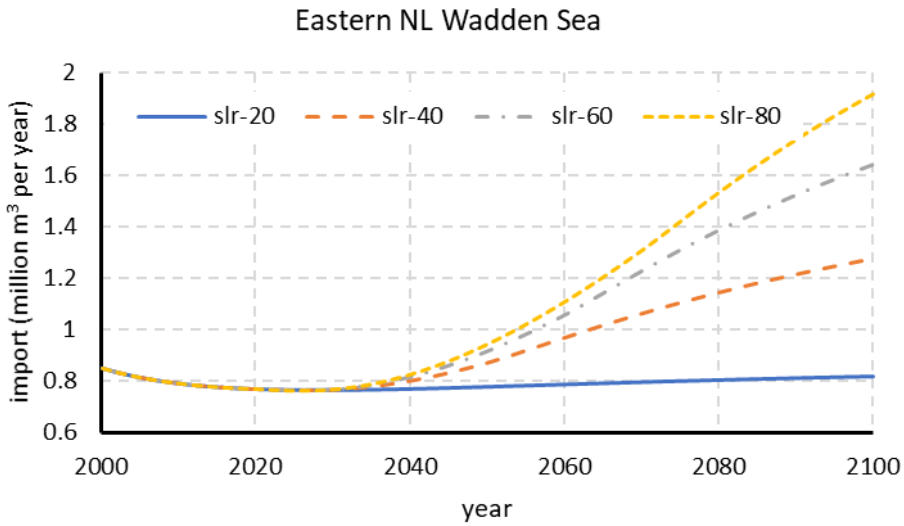

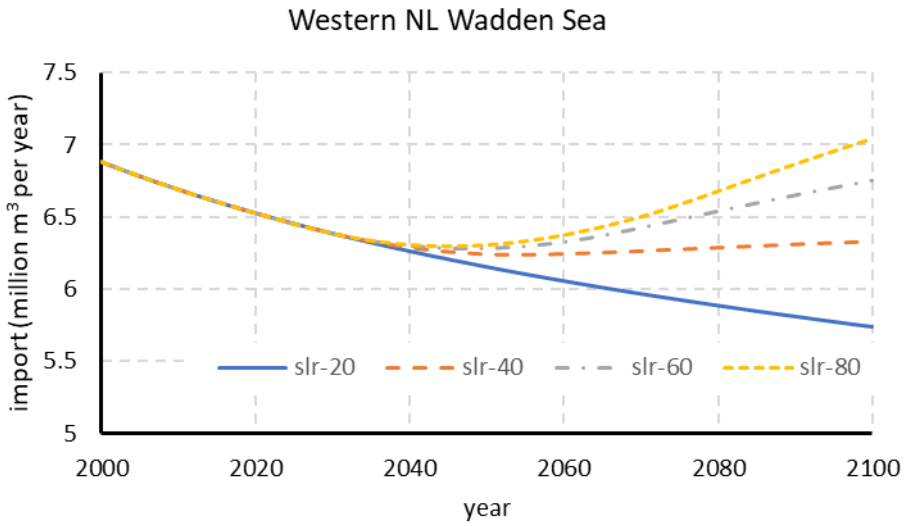

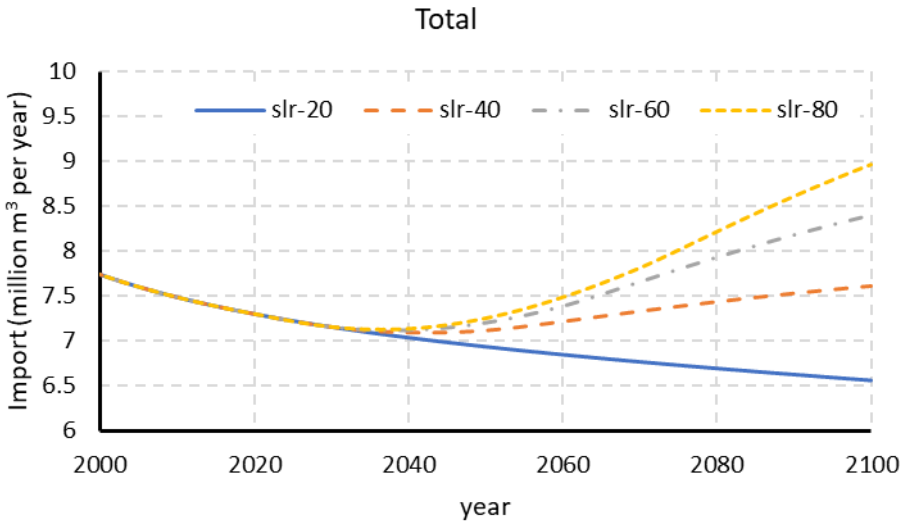

Figure 4.4 Total sediment import to the eastern part, the western part and the total Dutch Wadden Sea

The results suggest:

- The differences between the four SLR scenarios start in 2020, but the differences between the simulated import to the Wadden Sea basins start later. For the inlets Pinkegat and Erierlandse Gat the differences start to be noticeable from about 2030, i.e. 10 years later than those in the development of SLR. For Vlie and Zoutkamperlaag inlets this is 2050 and for Ameland Inlet 2045. For Texel Inlet the differences are not noticeable in the whole period until 2100. Apparently and as expected, there is a delay in response of the tidal inlet systems to the development of SLR. This delay depends on two factors, the size of the basin and the present morphological state. The larger the basin the longer the delay, this explains why the smaller systems (Pinkegat and Eierlandse Gat) respond first to the differences in development of SLR. The existing sediment demand in the basin due to human interference in the past can make the delay longer, which explains the longer delay of Zoutkamperlaag and the extreme long delay of Texel Inlet (the development of this tidal inlet system is almost fully controlled by the sediment demand due to the closure of the Zuiderzee).
- Considering the total sediment import to the whole Dutch Wadden Sea, the differences between the four scenarios do not become significant until about 2060 (Fig.4.4). The differences increase in time, but even in the remaining 40 years of the century the differences are relatively restricted: in 2100 the total import varies between 6.5 Mm^3/y (SLR-2) and 9 Mm^3/y (SLR-8). Note that the SLR rate varies with a factor 4 between the scenarios. The restricted differences are also due to the delayed response of the system to variation of SLR and due to the existing sediment demand caused by interferences in the past. This has two consequences:
    - Sensitivity of the model results to the exact variations of SLR in time (see previous Section) is expected to be limited.
    - The sediment import at the present state, for which the sediment budget results from the data analysis by Elias (2019) gives the best estimation, gives a good prediction for a long time in the future, despite the uncertain future SRL development. This means that the predictions of tidal flat losses by

extrapolating with constant sedimentation rate in the Dutch Wadden Sea by Wang et al. (2018) is reasonable. This emphasises also the importance of studying the present state using observations and process-based modelling.

- The differences between the three scenarios with SLR acceleration are relatively small compared with that between the lowest acceleration scenario SLR-4 and the scenario without acceleration of SLR (SLR-2). This can be explained by the time variations of sea-level according to the scenarios (Fig.4.1) and the delay in response of the system to SLR.

4.3 Improvement of the models

4.3.1 Eierlandse Gat Inlet

An obvious shortcoming in the model results presented in the previous Section concerns Eierlandse Gat. This is the only inlet through which sediment export has been taking place according to the observations (Elias et al., 2012; Wang et al., 2018). However, the model results suggest that sediment import is also taking place through this inlet. Apparently, no special calibration for this tidal inlet has been carried out in the past. A closer look at the model input for this inlet (Table 4.1) learned that this may be due to the too small tidal range used. The tidal range was set the same as in Texel Inlet although we know that the tidal range is increasing in the eastern direction. Therefore, the first attempt for improving the model is by setting the tidal range equal to the average between those in Texel Inlet and Vlie Inlet: (1.65+1.9)/2=1.78 m.

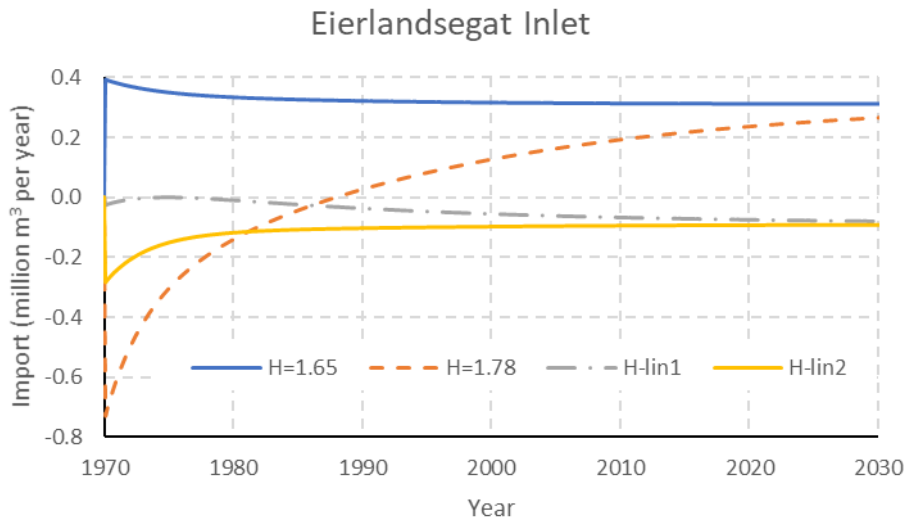

Figure 4.5 Influence of the development of tidal range in Eierlandse Gat. All simulations with constant SLR rate (2 mm/y). In the run H-lin1 the tidal range starts at 1.7 m in 1970 and increases with 3 mm/y. In the run H-lin2 the tidal range starts at 1.73 m and increases with the same rate (3 mm/y).

The results of the run with increased tidal range (=1.78 m) are shown in Figure 4.5. Initially, the sediment transport through the inlet became an export (about 0.78 Mm^3/y), but it quickly (within less than 20 years) turned to an import and it approaches to the same level as that according to the run with lower tidal range (=1.65 m). In both runs the import is approaching the dynamic equilibrium which is equal to the product of the SLR rate and the basin area. According to the observations, the sediment transport through this inlet has been an export for a long time (Elias et al., 2012; Wang et al., 2018). This cannot be reproduced by the model using a constant tidal range. Given the relations used for the morphological equilibrium in ASMITA, a constant export

through the inlet with rising sea-level can only be possible if the tidal prism is constantly increasing in time. An increase of the tidal prism can be caused by an increasing tidal range, a decreasing tidal flat volume, or an increasing basin area. According to the observations, the tidal flat volume in the basin has not been decreasing. Therefore, the only options left are increasing tidal range or increasing basin area. In the present version of ASMITA the horizontal areas of the morphological elements are constant in time, so it is not possible to simulate the situation with increasing basin area. Therefore, various scenarios of linearly increasing tidal range are simulated (see Fig.4.5 for two examples). From the results of these runs it is observed that the sediment transport through the inlet at the dynamic equilibrium depends on and is quite sensitive to the increase rate of the tidal range. It is indeed possible to keep a constant export with a rising sea-level and increasing tidal range. The increasing tidal range causes increase of the tidal prism with as consequence that the equilibrium volumes of the channels in the basin and the ebb-tidal delta increase. The sediment demand on the ebb-tidal delta and the sediment surplus in the channels caused by the increase of the tidal prism drive sediment transport from the channels to the ebb-tidal delta, export thus.

The scenario H-lin2 (tidal range starts at 1.73 m and increases with 3 mm per year) shown in Figure 4.5 is used to simulate all four SLR scenarios. The results of these simulations are shown in Figure 4.6. The relative differences between the scenarios show the same behaviour as in the existing runs (Figure 4.3), although the import rates in all scenarios are now lower. In the SLR-20 (continuation of the present SLR rate 2 mm/y) scenario this is even an export, but in all three accelerating SLR scenarios this export will turn to an import, somewhere between 2040-2050 depending on the scenario. Furthermore, it should be noted that the contribution of this inlet to the total sediment exchange between the North Sea coast and the Dutch Wadden Sea is limited.

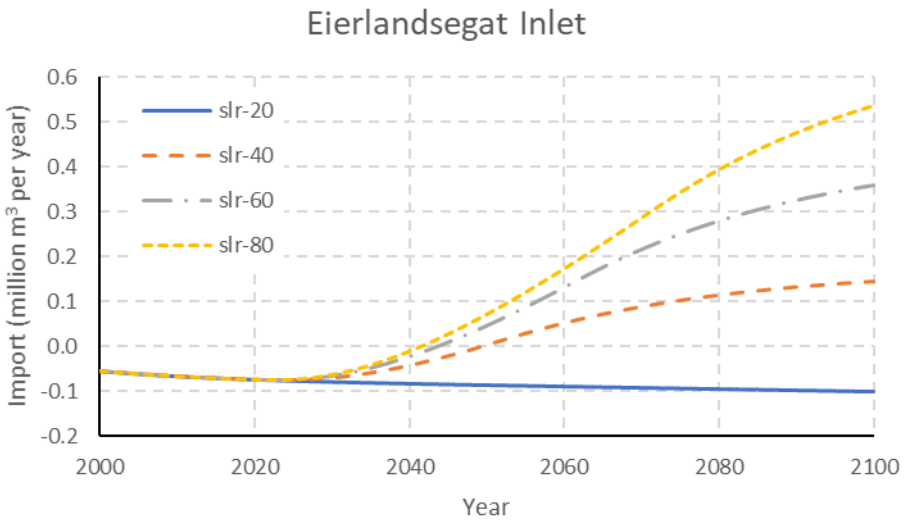

Figure 4.6 Results of the four scenarios with the setting of H-lin2.

4.3.2 Texel Inlet and Vlie

The two large inlet systems in the western Dutch Wadden Sea, Texel Inlet and Vlie, interact with each other because of the water and sediment exchange between them. The tidal divide between them is not a closed boundary between them and it is not fixed in position since the closure of the Zuiderzee (see Wang et al., 2013). Therefore, these two Inlet systems are

considered together here, although they are modelled as separate tidal inlet systems with ASMITA.

The closure of the Zuiderzee was a major human interference that caused a substantial disturbance with respect to the morphological equilibrium in the Texel Inlet – Vlie system. This disturbance and the decay in time of it has drawn a lot of attention in research based on data analysis as well as modelling. The continues research have resulted into changing insights into the behaviour of the system. In the time when the first version of the ASMITA models for these inlets were set up (end last century) the insight was that major part of the disturbance caused by the closure of the Zuiderzee was already damped out. Therefore, the first parameter setting of the models were such that the imports through the two inlets were at a relatively low level. Later, Elias (2006) concluded that the disturbance was far from damped out and there is still a large sediment demand in the back-barrier basins of the inlets. Important motivation for this is that the sediment import through especially the Texel Inlet, determined from the data analysis, had been more or less constant in time and at a high level. Based on this insight the parameter setting of the Texel Inlet ASMITA model had been changed (Wang et al., 2006) in order to reproduce the higher sediment import rate. An extra support for the change was the fact that the parameters for defining the morphological equilibrium just need to be set to closer to the normal values. However, the newest insight from the data analysis (Elias, 2019) is that at present the import rate (determined via the recent trend of changes) through Texel Inlet has become lower than the long-term averaged rate (based on long-term trend). On the other hand, the import rate through the Vlie Inlet is higher than according to the ASMITA model (Figure 4.3). Therefore, an attempt is made to update the parameter setting for the ASMITA models for these two inlets, in order to make the model results more consistent with the newest insights.

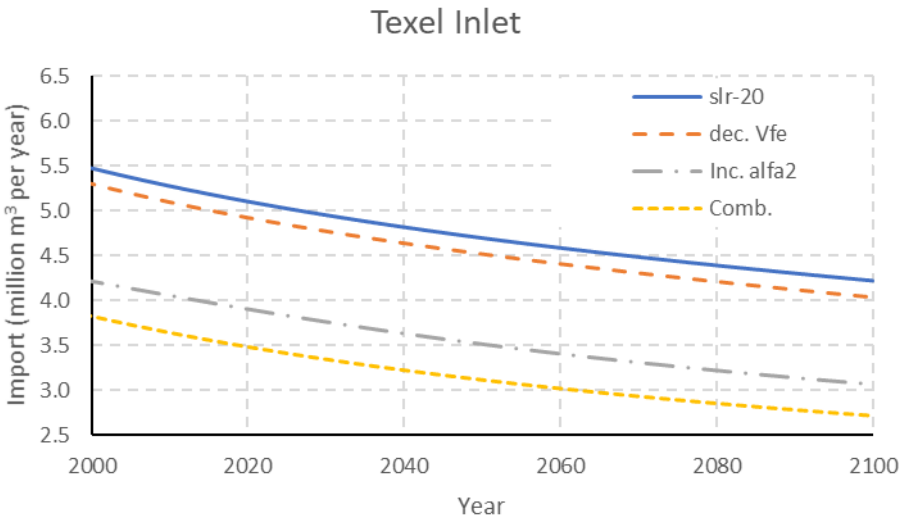

Figure 4.7 Sediment import through Texel Inlet simulated with ASMITA using various parameter settings. Run 'SLR-20' is the reference run as reported in 4.2, In run 'dec. Vfe' the equilibrium tidal flat volume V_{fe} is decreased, in run 'Inc. alfa2' the coefficient in the relation for the equilibrium channel volume α_c is increased, and in run 'Comb.' the two changes are combined.

According to the newest insights the modelled sediment import through Texel Inlet needs to decrease and that though Vlie needs to increase. The effective way to do so is changing the parameters determining the morphological equilibrium in the basin, i.e. the equilibrium volume of tidal flat V_{fe} and the coefficient in the relation for the equilibrium channel volume α_c. In the last update of the parameter setting for Texel Inlet V_{fe} was increased following the empirical

relations (2-13) through (2-16) that determine V_{fe} from the basin area A_b and the tidal range. However, the horizontal area of the tidal flat A_f in the basin of Texel Inlet is relatively small (see Table 4.1), and it is fixed in the present ASMITA model. This has the consequence that the (effective) equilibrium height of the tidal flat is relatively high, almost 70% of the tidal range instead of around 40% according to (2-14). Therefore, first V_{fe} is decreased such that the effective equilibrium height of the tidal flat is 40% of the tidal range (V_{fe}=87.78 million m^3 instead of 151 million m^3). Note that this change also has consequences for the equilibrium of the channel and the ebb-tidal delta, because a smaller tidal flat volume means a larger tidal prism. This change indeed decreases the sediment import (Figure 4.7), but the effect is limited. Therefore, it is decided also to increase α_c (from 10*10^{-6} to 15*10^{-6}). A motivation from this is that although potentially some of the subtidal areas (belonging to the channel element thus) should change to intertidal areas (flat) the change does not happen because flow is still strong enough for preventing the deposition of fine sediment. In other words, the potential sediment demand according to the empirical relations is not becoming real effective sediment demand. This also motivate the lowering of the V_{fe} value. The results of the run with increased α_c value and of the run with the two changes combined are also shown in Figure 4.7. It is noted that the effect of the lowering of V_{fe} is dependent on the value of α_c because of its effect on the tidal prism. The run with the two changes combined will further be used for simulating the scenarios of accelerated SLR.

A similar reasoning concerning the V_{fe} value can be made for the Vlie Inlet, with the opposite effect. According to the existing parameter setting (Table 4.1) the effective equilibrium height of tidal flat is about 30% of the tidal range. This is changed to about 40% (V_{fe} increased from 190 to 250 million m^3). The effect of this change is illustrated in Figure 4.8. The model results after this change is already more or less in line with the present insight (Elias, 2019). Therefore, this run is used to do the simulations for the other SLR scenarios.

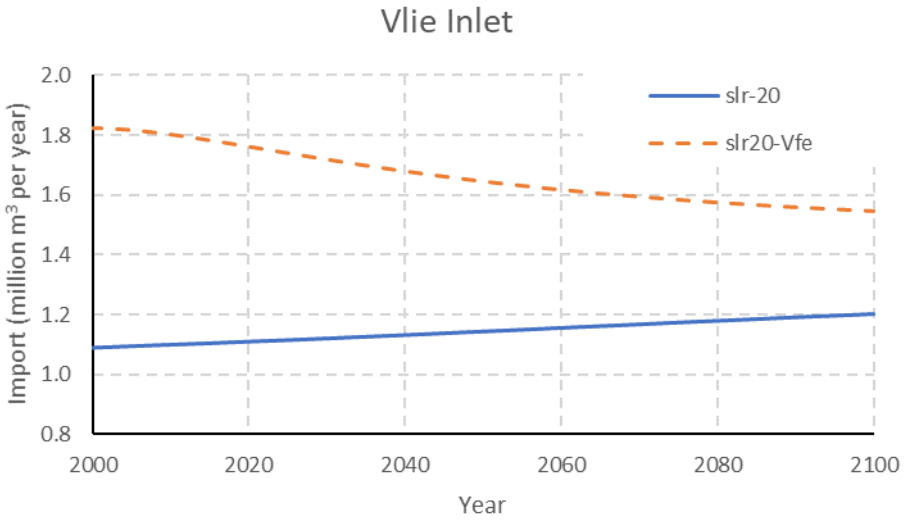

Figure 4.8 Sediment import through Vlie Inlet simulated with ASMITA using two different parameter settings. Run 'SLR-20' is the reference run as reported in 4.2, In run 'SLR20-Vfe' the equilibrium tidal flat volume V_{fe} is increased.

The results of the simulations for all four SLR scenarios are shown in Figure 4.9 for Texel Inlet and in Figure 4.10 for Vlie. For Texel Inlet an effect of the changed parameter setting is that the differences between the scenarios become clearer, in addition to the lower import rate for all scenarios. This can be explained by the lowered effective sediment demand in the basin, so

SLR becomes relatively more important. For Vlie the import rate becomes higher for all scenarios and the relative differences between the scenarios are not changed much.

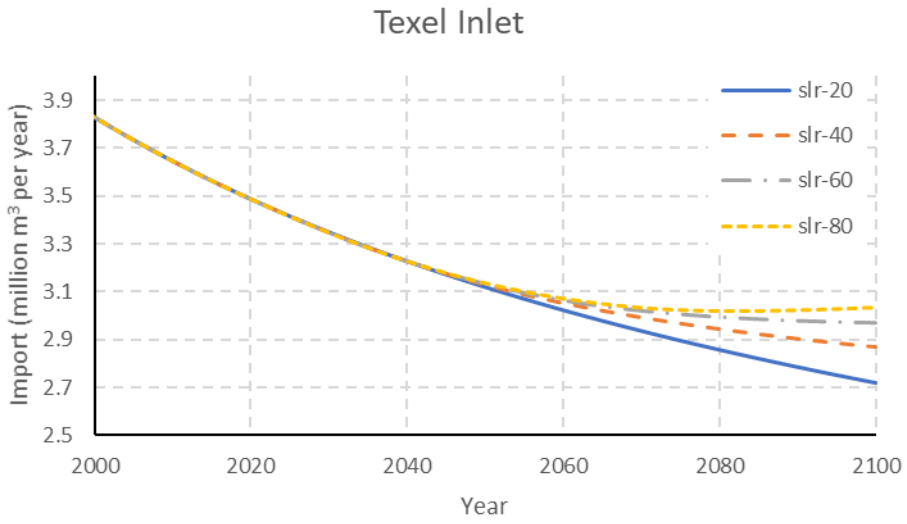

Figure 4.9 Simulated sediment import through Texel Inlet after changing the parameter setting.

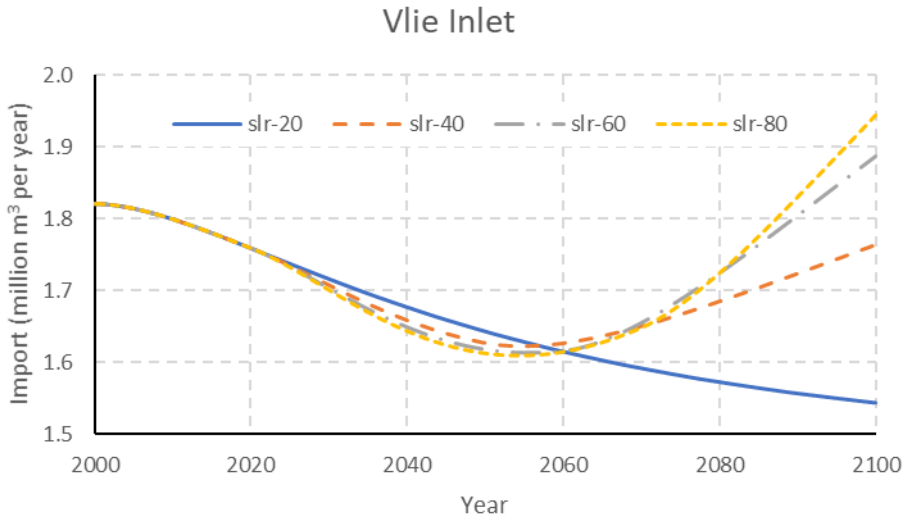

Figure 4.10 Simulated sediment import through Vlie Inlet after changing the parameter setting.

4.3.3 Results updated runs

The results of the simulations after updating the parameter settings (in the western part) are summarised in Figure 4.11. The total import to the Dutch Wadden Sea is changed (lower) but the conclusions concerning the differences between the scenarios remain unchanged (see 4.2). This means that an extensive calibration of the models to reproduce the sediment imports through the tidal inlets more accurately is not crucial to draw the relevant conclusions concerning coastal nourishment. Therefore, the parameter settings for the three inlets in the eastern part of the Dutch Wadden Sea are not updated in the present study.

For the long-term coastal nourishment strategy, the following conclusions are most relevant:

- The effect of acceleration of SLR on the sediment import (thus loss from the coast) will not be noticeable before 2040, even if the acceleration starts in 2020.
- The differences between the scenarios concerning sediment import to the Wadden Sea is much less than the difference in SLR rate might suggest until 2100. The import rate varies between 5 and 7.5 million m^3 among the four scenarios with SLR rate changing between 2 and 8 mm/y.
- No substantial increase of sediment import to the Wadden Sea is expected until 2100. The import rate first decreases in time if the present SLR rate continues, because of the damping of the disturbance due to interferences in the past. The acceleration of SLR will change this decrease trend, but not until 2050 according to all scenarios. For the highest SLR scenario simulated, the import rate will increase with about 1.5 million m^3 per year in 2100 compared to the present.

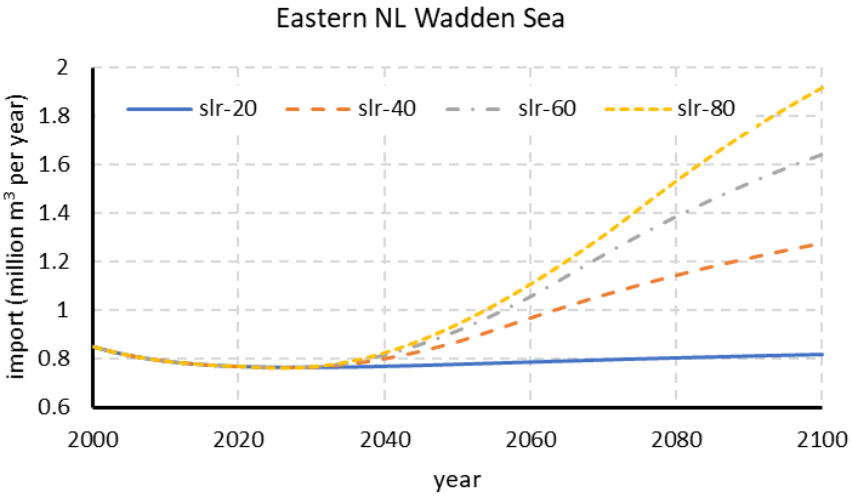

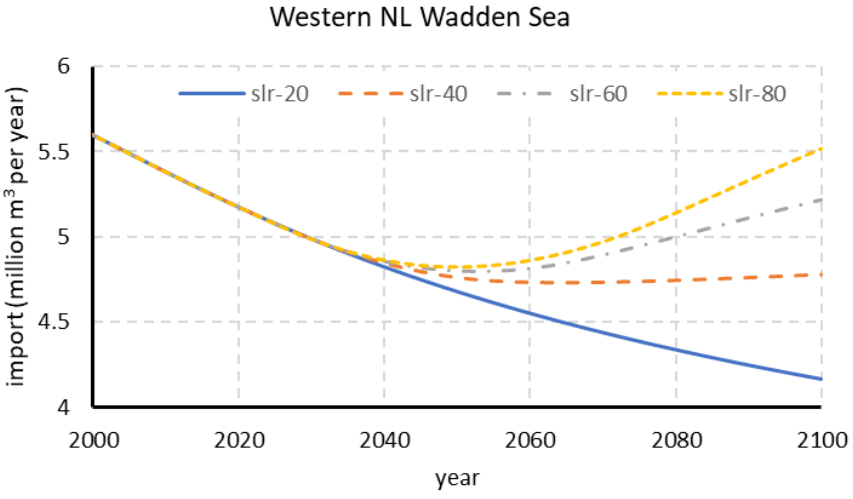

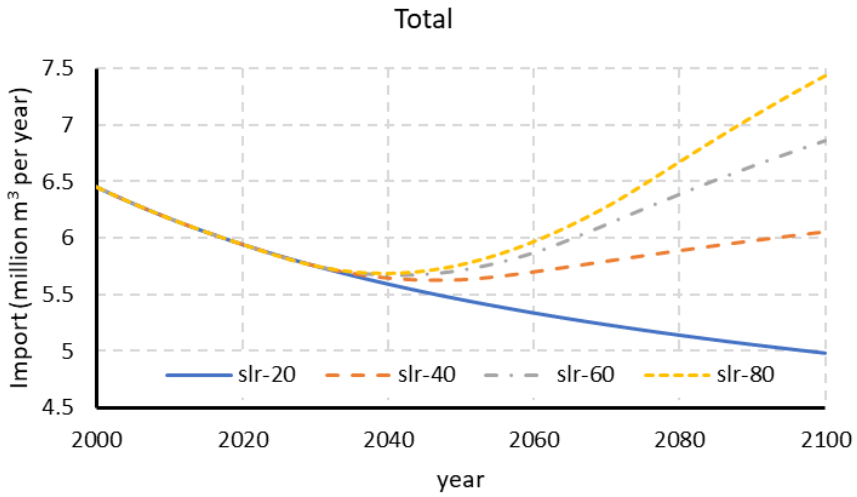

Figure 4.11 Simulated sediment import to the eastern part, western part and the whole Dutch Wadden Sea for the four SLR scenarios using ASMITA models with updated parameter setting in the western part.

5 Concluding discussions

5.1 Updating of the ASMITA models

The ASMITA models used in the PONTOS-ASMITA modelling study for the Netherlands coast (Wang et al., 2006) form the starting point of the present study. These models are used to carry out the base simulations for the four SLR scenarios. The simulations are run over the period 1970-2100, and therefore include a part hindcasting and a part forecasting. Based on the comparison between the hindcasting results and the newest insights from the analysis of historical development (Elias, 2019) the models for the three tidal inlet systems, Vlie, Eierlandse Gat and Texel Inlet, have been updated.

In order to reproduce the export of sediment through the Eierlandse Gat, as concluded from all data analysis studies, the prescribed tidal range for this model is updated. Its initial value is increased, and more importantly, it is set to be linearly increasing in time. The linear increasing trend is necessary to maintain a sediment export from the basin under influence of SLR. Prescribing a constant larger value of the tidal range results in an export at the beginning of the simulated period, but the system then develops to the dynamic equilibrium in which sedimentation in the basin (thus import) is balancing the SLR. For this relatively small tidal inlet with relatively small morphological timescales, the initial export cannot maintain for a long time as the results of the data analysis indicate. It is also important to note that the model results are quite sensitive to the linear increasing rate of the tidal range.

For the Texel Inlet the parameter setting in the ASMITA model was updated in 2006 following the insights from the study of Elias (2006). The parameters in the relations defining the morphological equilibrium in the basin were changed such that the sediment demand of the basin became much larger. This had the consequence that the sediment import through the inlet maintains at a high level for a long time, in the past and for the future. In the changed setting the parameters are close to the “normal” values. However, according to the latest analysis of the historical development (Elias, 2019) the sediment import through the inlet is substantially lower compared to the long-term trend. Apparently, the potential sediment demand has not fully become effective sediment demand in the basin of this inlet. Following the newest insight parameter setting is partly changed back, such that the sediment demand in the basin becomes lower. This is achieved by lowering the equilibrium volume of the intertidal flat and increasing the coefficient in the relation for the equilibrium channel volume. After the changes the equilibrium height in the prescribed (horizontal) area of intertidal flat became in agreement with the known empirical relation. The increased equilibrium channel volume is necessary to reproduce the effective sediment demand rather than the potential sediment demand.

For the Vlie Inlet the morphological equilibrium in the basin also need to be changed by updating the parameter setting, but now in opposite direction. The sediment demand in the basin needs to be increased, because the sediment import rate according to the data analysis is higher than simulated by the existing ASMITA model. For this inlet, changing the equilibrium intertidal flat volume such that the equilibrium flat height in the prescribed area equal to the value according to the empirical relation appeared to be sufficient to make the model results in line with the newest insights.

5.2 Model results

Four future SLR scenarios are considered in this modelling study, with SLR rate equal to 2, 4, 6 and 8 mm/y in 2100 respectively. For the time process of how the SLR is changing from the present rate to the rate in 2100 reference is made to the scenarios described by Vermeersen et al. (2018). In all four scenarios the SLR is constant and equal to 2 mm/y until 2020. In the three accelerating scenarios the SLR rate increases then linearly in time to the maximum (2100) value and then remain constant again. The increasing period to achieve the 2100 value is until 2050 for the 4 mm/y scenario, until 2060 for the 6 mm/y scenario and until 2070 for the 8 mm/y scenario. The four scenarios are simulated with the existing as well as the updated ASMITA models for the six tidal inlet systems: Zoutkamperlaag, Pinkegat, Ameland Inlet, Vlie, Eierlandse Gat and Texel Inlet.

The parameter settings of the three inlets in the western part of the Dutch Wadden Sea have been updated. This turned the import through Eieralndse Gat to an export, decreased the import rate through Texel Inlet, and increased the import rate through Vlie Inlet, following the newest insights concerning the present state of the system. However, further comparison between the results from the existing models and those from the updated models learned that the effect of the updating of the models is very limited concerning e.g. the differences between the scenarios. This implies that more extensive calibration of the models is not necessary for the present study. Possible insufficient calibration would mean that an uncertainty concerning the sediment exchange between the Wadden Sea and the North Sea coasts at present, but this uncertainty can be eliminated by using the results from the data analysis.

The differences in SLR between the four scenarios start in 2020, but the differences in the simulated sediment transport through the inlets between the scenarios start later, with a delay. The delay depends on the morphological timescales, so it is smaller for the smaller inlet systems than for the larger systems. The delay depends also on present state of the system concerning in how far the system is deviated from the (dynamic) morphological equilibrium, so it e.g. becomes very large for the Texel Inlet with a large existing sediment demand. The combined effects of these two factors resulted in a delay such that the start time of noticeable differences between the scenarios varies from 2030 for the Pinkegat and Eierlandse Gat to end of the century for Texel Inlet. The delayed effects of the changing SLR can better be understood with the help of the results of the theoretical analysis (Chapter 3), from which it was concluded that the timescale for achieving the dynamic morphological equilibrium is proportional to the morphological timescale with respect to morphological equilibrium (without SLR) and increases non-linearly with the SLR rate.

For the total sediment import to the six tidal basins together the differences between the four SLR scenarios will not become significant until 2060 and remain restricted until 2100. The difference between the highest and the lowest scenario in 2100 is in the order of 2.5 million m^3 per year, while the SLR rate in the highest scenario is 4 times that in the lowest scenario. In all scenarios the total import will be decreasing until about 2040 according to the model results, due to the decay of the disturbance to morphological equilibrium caused by the interferences in the past. In the three accelerating scenarios the import will turn to an increasing trend, resulting in a higher import rate than at present. However, the difference between the total import rates in 2100 and 2020 will be limited according to the model results. Even for the highest SLR scenario the increase is less than 2 million m^3 per year.

The different tidal basins in the Wadden Sea will respond very differently when SLR accelerate, as the SLR rate will be the same but the critical SLR rate for drowning is very different for the different basins. In Table 5.1 the critical SLR rates for the six tidal basins in the Dutch Wadden Sea, as calculated by Wang et al. (2018) are given together with the dimensionless SLR rate r for four SLR rates (2, 4, 6 and 8 mm/y). The results from the theoretical analysis concerning

the dynamic morphological equilibrium and the morphological timescale for achieving the dynamic equilibrium are helpful for the interpretation of the model results.

Table 5.1 Critical SLR rate for drowning of the various tidal inlet systems in the Dutch Wadden Sea from Wang et al. (2018) and the dimensionless SLR rate r for four different SLR rates (2, 4, 6 and 8 mm/y).

Inlet	A_b (m^2)	R_c (mm/y)	*r for SLR rate =*			
			2 mm/y	*4 mm/y*	6 mm/y	8 mm/y
Texel	655	7.00	0.29	0.57	0.86	1.14
ELGT	157.7	18.0	0.11	0.22	0.33	0.44
Vlie	715	6.30	0.32	0.63	0.95	1.27
Amel	276.3	10.4	0.19	0.38	0.58	0.77
PinkeG	49.6	32.7	0.06	0.12	0.18	0.24
ZoutK	105	17.1	0.12	0.23	0.35	0.47

5.3 Uncertainties

There are various sources of uncertainties in the presented model results. First and as already mentioned, the models have not been extensively calibrated for reproducing the development since 1970. However, it has been shown that this has practically no effect on the model results concerning e.g. the differences between the SLR scenarios. This uncertainty can be overcome by using the results from the data analysis for the quantitative import rate and using the model results for the future developments.

A major uncertainty concerns the SLR development itself, as indicated by the four very different scenarios. However, the model results indicate that the effects of these differences on the sediment import to the Wadden Sea are relatively limited. This makes the uncertainty in the conclusions relevant for the management much less. This means also that the uncertainty introduced in the exact definition of the scenarios, i.e. how the acceleration of SLR takes place in time, is limited.

The remaining source of uncertainties is due to the shortcomings of the models as summarized in Chapter 2.5. By considering the tidal divide as fixed and closed boundaries between the basins and fixing the internal distribution between subtidal and intertidal part during the simulation the sediment demand in a basin is influenced. The effect on the model results can be indicated by varying the parameters in the relations for the morphological equilibrium as done by updating the models for Texel Inlet and Vlie. The conclusion that the update does not significantly influence the model results concerning the relative differences implies that the uncertainty corresponding to these shortcomings is limited.

The uncertainty due to the shortcoming that the change of tidal range due to morphological development of the system is not accounted for is more important. This is because of the sensitivity of the model results to the increasing rate of tidal range, as shown during the updating of the model for Eierlandse Gat (see Section 4.3). Acceleration of SLR is expected to increase the tidal range in the Wadden Sea. According to the results for the Eierlandse Gat an increasing tidal range results into a lower import (c.q. higher export) rate.

Another shortcoming of the models is due to the single fraction sediment transport module. However, as Wang and Van der Spek (2015) explained, the parameter settings of the models in fact do take into account the effect of sand-mud mixture in the system, limiting the corresponding uncertainty. On the other hand, the theoretical analysis (Chapter 3) shows that

the value of the power *n* influences the critical SLR rate for drowning for the same morphological timescale (related to decay of disturbances with respect to the morphological equilibrium without SLR). Wang et al. (2008) showed that the used value (*n*=2) is too low. According to the theoretical analysis this results in a too high critical rate of SLR, implying that errors are introduced in the model results at the very large timescale (related to the drowning process). However, the simulated period (until 2100) is relatively small to this timescale. Therefore, the uncertainty corresponding to this shortcoming is considered as limited.

5.4 Relevance for management

For the long-term coastal nourishment strategy, the following conclusions are most relevant:

- The effect of SLR acceleration on the sediment import to the Wadden Sea (thus loss from the coast) will not be noticeable before 2040, even if the acceleration starts in 2020.
- The differences between the scenarios concerning sediment import to the Wadden Sea is much less than the difference in SLR rate might suggest until 2100. The difference in import rate between the highest (8 mm/y) and lowest (2 mm/y) scenarios is only about 2.5 million m^3 per year in 2100, varying from about 5 million m^3 per year (for the lowest scenario) to about 7.5 million m3 per year.
- No substantial increase of sediment import to the Wadden Sea is expected until 2100. The import rate first decreases in time if the present SLR rate continues, because of the damping of the disturbance due to interferences in the past. The acceleration of SLR will change this decrease trend, but not until 2050 according to all scenarios. For the highest SLR scenario (8 mm/y) simulated, the import to the eastern part of the Dutch Wadden Sea increases with 140% and that to the western part increases with 35%. For the whole Dutch Wadden Sea the total import rate will increase with about 1.5 million m^3 per year in 2100 compared to at present (about 6 million m3 per year), i.e. an increase of about 50%.

In conclusion, the effect of accelerating SLR on the loss of sand from the coastal zone due to import to the Wadden Sea will be limited until 2100.

The limited effect of changing SLR on the sediment import to the Wadden Sea can be considered as positive for the maintenance of the coasts by nourishment, but it is negative for the conservation of the ecological value of the Wadden Sea. Acceleration of SLR can thus cause more loss of intertidal flat area than one might expect. However, according to the data analysis the sedimentation rate in the Dutch Wadden Sea has been higher than the SLR rate. In fact, the way in which Wang et al. (2018) projected the development of the tidal flat area in the future has been proven to be far from wrong, although the sedimentation rate used for the extrapolation needs to be updated with the new insights. The model results indicate that the extrapolation (using correct sedimentation rate) causes a little bit too optimistic projection for the near future (until 2050) and a bit too pessimistic projection for the far future (beyond 2050) for the considered accelerating SLR scenarios.

The theoretical analysis presented in Chapter 3 indicates that it will be practically impossible to identify if a tidal basin is drowning due to accelerated SLR. A tidal inlet system would behave in the same way when SLR rate is relatively high, no matter if it is below, equal or above the critical limit for drowning. Even if the SLR rate is not close to the critical limit, the delayed response of the tidal inlet system will cause some loss of the intertidal flat area, and the large

timescale for achieving new dynamic morphological equilibrium makes monitoring effect of accelerated SLR a challenging task.

5.5 Recommendations

Concerning management of the Wadden Sea system the following recommendations are made:

- Study nourishment strategies for influencing sediment import. Given the uncertain future development of SLR and the different (maybe even conflicting) effects of sediment import to the two management issues, coastal maintenance and conservation of ecological value in the Wadden Sea, it is desirable to be able to influence the import rates through the inlets. Nourishments on e.g. the ebb-tidal deltas are the possibilities to be considered.
- Combine field observation with modelling for monitoring effects of (changing) SLR. Development of SLR itself can be well monitored via field measurements, but combination with modelling will be needed to conclude if certain limit (for e.g. drowning) will be exceeded.
- For a best estimate of the current import of the Wadden Sea Sytem it is advised to use the results of the data analysis of Elias et al, 2019.

Recommendations concerning research to the Wadden Sea system in general:

- More emphasis on the determination of import rates through the various tidal inlets by combining data analysis and modelling of hydrodynamic and sediment transport processes is recommended. The present rate of import to the Wadden Sea will be a good prediction for a long time (decades) in the future and it is the main uncertain part in the development.
- Investigate the development of the tidal divide areas in the Wadden Sea. In the ASMITA modelling the tidal inlets are considered as isolated systems, assuming that the tidal divides form the closed boundary between the tidal basins. Whether this assumption is justified depends on the development of the tidal divides responding to the changing SLR.
- Investigate the development of the tidal range in the tidal basins in relation to the morphological changes. According to the model results, the development of the sediment exchange between the North Sea coasts and the Wadden Sea is sensitive to the development of the tidal range in the Wadden Sea. In the ASMITA modelling the change of the tidal range corresponding to SLR and morphological development is not taken into account. Therefore, the investigation needs to be carried out with data analysis for the past, and with process-based models for the future.
- Investigate expected dynamic equilibrium states for all Wadden Sea (and Western Scheldt) basins.

Recommendations concerning ASMITA modelling:

- Extend the present modelling study, which only focuses on the sediment exchange through the inlets, by analyzing the development of the morphological elements (ebb-tidal delta, channels and intertidal flats in the basin) of the various tidal inlet systems.

- Improving ASMITA by implementing graded sediment transport module, at least by including a sand and a mud fraction. This is important for better prediction of the critical SLR rate for drowning as indicated by the theoretical analysis, and also important for understanding the behavior of the tidal inlet systems responding to accelerating SLR determined by the dimensionless SLR rate.
- Extend the ASMITA models for the tidal inlet systems by including a saltmarsh in the back-barrier basin as an additional morphological element. This is especially important after improving ASMITA with a mud transport.
- Extend the present three-elements schematization of the ASMITA models by dividing the basins into more subparts, based on e.g. the insights from the analysis of Elias (2019). Most important thing for this extension is the applicability of the empirical relations for the morphological equilibrium for the subparts of the basins.

Combine with process-based modelling for e.g. better setting for the parameters influencing the morphological timescales.

6 References

Buijsman, M.C., 1997, The impact of gas extraction and sea-level rise on the morphology of the Wadden Sea, WL | Delft Hydraulics, Report H3099.30.

Elias, E.P.L., Van der Spek, A.J.F., Wang, Z.B. & De Ronde, J.G., 2012. Morphodynamic development and sediment budget of the Dutch Wadden Sea over the last century. Netherlands Journal of Geoscience 91: 293-310.

Elias, E.P.L., 2018, Rapport data analyse westelijk deel NL Waddenzee.

Elias, E.P.L., 2019, Rapport data analyse oostelijk deel NL Waddenzee.

Elias, E.P.L. (2019). Een actuele sedimentbalans van de Waddenzee. Deltares rapport, 11203683-001-ZKS-0002, Deltares, Delft, 83p.

Townend, I.H., Wang, Z.B., Stive, M.J.F. & Zhou, Z., 2016a. Development and extension of an aggregated scale model: part 1 Background to ASMITA. China Ocean Engineering 30: 483-504.

Townend, I.H., Wang, Z.B., Stive, M.J.F. & Zhou, Z., 2016b. Development and extension of an aggregated scale model: part 2 Extensions to ASMITA. China Ocean Engineering 30: 651-670.

Van Maanen, B., Coco, G., Bryan, K.R., Friedrichs, C.T., 2013, Modeling the morphodynamic response of tidal embayments to sea-level rise. Ocean Dynamics 63: 1249. https://doi.org/10.1007/s10236-013-0649-6.

Wang, Z.B., Elias, E.P.L., Van der Spek, A.J.F. & Lodder, Q.L., 2018. Sediment budget and morphological development of the Dutch Wadden Sea - impact of accelerated sea-level rise and subsidence until 2100. Netherlands Journal of Geosciences, 97-3: 183-214.

Cowell P J, Stive M J E, Niedoroda A, De Vriend H J, Swift D, Kaminsky G M and Capobianco M, 2003, The coastal-tract (part 1): A conceptual approach to aggregated modelling of low-order coastal change. Journal of Coastal Research, 19 (4), 812-827.

Di Silvio G, 1989, Modelling the morphological evolution of tidal lagoons and their equilibrium configurations, IAHR Congress, pp. C-169-C-175, IAHR.

Di Silvio G, Dall'angelo C, Bonaldo D and Fasolato G, 2010, Long-term model of planimetric and bathymetric evolution of a tidal lagoon. Continental Shelf Research, 30 (8), 894-903.

Eysink, W.D., 1990. Morphological response of tidal basins to changes. In: B.L. Edge (ed.), "Coastal engineering 1990 Proc.", ASCE, New York, p. 1948-1961.

Eysink, W.D., et al, 1998, Effecten van bodemdaling door gaswinning in en rond de Waddenzee, Morfologie, infrastructurele en economische aspecten. WL | Delft Hydraulics, Rapport H3099.

Gallappatti G and Vreugdenhil C B, 1985, A depth integrated model for suspended sediment transport. Journal of Hydraulic Research, 23 (4), 359-375.

Kragtwijk, N.G., 2002. Aggregated Scale Modelling of Tidal Inlets of the Wadden Sea. Report 22822/DC03.01.03b. Delft, The Netherlands: WL I Delft Hydraulics/ Delft Cluster

Kragtwijk N G, Stive M J F, Wang Z B and Zitman T J, 2004, Morphological response of tidal basins to human interventions. Coastal Engineering, 51, 207-221.

Lacey G, 1930, Stable channels in alluvium. Minutes of the Proceedings of the Institution of Civil Engineers, 229, 259-292,doi: 10.1680/imotp.1930.15592.

Langbein W B, 1963, The hydraulic geometry of a shallow estuary. Bulletin of Int Assoc Sci Hydrology, 8 (3), 84-94.

Leopold L B and Langbein W B, 1962, The concept of entropy in landscape evolution, Report No: Professional Paper 500-A, pp. A1-A20, Survey U G, United States Government Printing Office, Washington.

O'connor B A, Nicholson J and Rayner R, 1990, Estuary geometry as a function of tidal range, International Conference of Coastal Engineering, pp. 3050-3062, American Society of Civil Engineers.

Spearman J, 2007, Hybrid modelling of managed realignment, Report No: TR157, p. 100, Wallingford, UK.

Stive M J F, Capobianco M, Wang Z B, Ruol P and Buijsman M C, 1998, Morphodynamics of a tidal lagoon and adjacent coast, Dronkers J and Scheffers M B a M(eds), Physics of Estuaries and Coastal Seas: 8th International Biennial Conference on Physics of Estuaries and Coastal Seas, 1996, pp. 397-407, A A Balkema.

Stive M J F and Wang Z B, 2003, Morphodynamic modelling of tidal basins and coastal inlets, In: Advances in coastal modelling, Series, Vol, Lakkhan C (ed), pp. 367-392, Elsevier Sciences, Amsterdam.

Townend I H, Wang Z B and Rees J G, 2007, Millennial to annual volume changes in the humber estuary. Proc.R.Soc.A, 463, 837-854.

Townend I H, Wang Z B, Stive M J E and Zhou Z, 2016, Development and extension of an aggregated scale model: Part 1 – background to asmita. China Ocean Engineering, 30 (4), 482-504.

Van Geer, P., 2007, Long-term modelling of the Western part of the Dutch Wadden Sea, Report Z4169, WL | Delft Hydraulics.

Van Goor. M.A.. 2001. Influence of Relative Sea Level Rise on Coastal Inlets and Tidal Basins. ReportZ2822/DC03.01.03a. Delft, The Netherlands: WL I Delft Hydraulics/Delft Cluster

Van Goor M A, Zitman T J, Wang Z B and Stive M J F, 2003, Impact of sea-level rise on the morphological equilibrium state of tidal inlets. Marine Geology, 202, 211-227.

Van Rijn L C, 1993, Principles of sediment transport in rivers, estuaires and coastal seas, Aqua Publications, Amsterdam.

Walton T D and Adams W D, 1976, Capacity of inlet outer bars to store sand, Fifteenth Coastal Engineering Conference, pp. 1919-1936, American Society of Civil Engineers.

Wang Z B, 1992, Theoretical analysis on depth-integrated modelling of suspended sediment transport. Journal of Hydraulic Research, 30 (3), 403-420.

Wang, Z.B., Steetzel, H. en M. van Koningsveld, 2006, Effecten van verschillende scenarios van kustonderhoud, Resultaten lange-termijn simulaties morfologische ontwikkeling Nederlandse Noordzeekust, WL | Delft Hydraulics, Rapport Z4051.

Wang Z B, De Vriend H J, Stive M J F and Townend I H, 2008, On the parameter setting of semi-empirical long-term morphological models for estuaries and tidal lagoons, Dohmen-Janssen C M and Hulscher S J M H(eds), River, Coastal and Estuarine Morphodynamics, pp. 103-111, Taylor & Francis.

Wang Z B, Karssen B, Fokkink R J and Langerak A, 1998, A dynamic-empirical model for estuarine morphology, In: Physics of estuaries and coastal seas, Series, Vol, Dronkers J and Scheffers M B a M (eds), pp. 279-286, Balkema, Rotterdam.

Wang Z B and Townend I H, 2012, Influence of the nodal tide on the morphological response of estuaries. Marine Geology, 291-294, 73-82.

Winterwerp J C and Van Kesteren W G M, 2004, Introduction to the physics of cohesive sediment in the marine environment, Elsevier, Amsterdam.

Wright A D and Townend I H, 2006, Predicting long term estuary evolution using regime theory, Littoral 2006 Conference Proceedings, pp. 1-9, Gdansk University of Technology, Faculty of Management and Economics, Traugutta 79.